THE ASTROPHYSICAL JOURNAL, 594:1–24, 2003 September 1

COSMOLOGICAL RESULTS FROM HIGH-z SUPERNOVAE[1,2]

JOHN L. TONRY,[3] BRIAN P. SCHMIDT,[4] BRIAN BARRIS,[3] PABLO CANDIA,[5] PETER CHALLIS,[6] ALEJANDRO CLOCCHIATTI,[7] ALISON L. COIL,[8] ALEXEI V. FILIPPENKO,[8] PETER GARNAVICH,[9] CRAIG HOGAN,[10] STEPHEN T. HOLLAND,[9] SAURABH JHA,[6,8] ROBERT P. KIRSHNER,[6] KEVIN KRISCIUNAS,[5,11] BRUNO LEIBUNDGUT,[12] WEIDONG LI,[8] THOMAS MATHESON,[6] MARK M. PHILLIPS,[11] ADAM G. RIESS,[13] ROBERT SCHOMMER,[5,14] R. CHRIS SMITH,[5] JESPER SOLLERMAN,[15] JASON SPYROMILIO,[12] CHRISTOPHER W. STUBBS,[10] AND NICHOLAS B. SUNTZEFF[5]

Received 2003 February 28; accepted 2003 May 6

ABSTRACT

The High-z Supernova Search Team has discovered and observed eight new supernovae in the redshift interval $z = 0.3$–1.2. These independent observations, analyzed by similar but distinct methods, confirm the results of Riess and Perlmutter and coworkers that supernova luminosity distances imply an accelerating universe. More importantly, they extend the redshift range of consistently observed Type Ia supernovae (SNe Ia) to $z \approx 1$, where the signature of cosmological effects has the opposite sign of some plausible systematic effects. Consequently, these measurements not only provide another quantitative confirmation of the importance of dark energy, but also constitute a powerful qualitative test for the cosmological origin of cosmic acceleration. We find a rate for SN Ia of $(1.4 \pm 0.5) \times 10^{-4}\ h^3\ \mathrm{Mpc}^{-3}\ \mathrm{yr}^{-1}$ at a mean redshift of 0.5. We present distances and host extinctions for 230 SN Ia. These place the following constraints on cosmological quantities: if the equation of state parameter of the dark energy is $w = -1$, then $H_0 t_0 = 0.96 \pm 0.04$, and $\Omega_\Lambda - 1.4\Omega_M = 0.35 \pm 0.14$. Including the constraint of a flat universe, we find $\Omega_M = 0.28 \pm 0.05$, independent of any large-scale structure measurements. Adopting a prior based on the Two Degree Field (2dF) Redshift Survey constraint on Ω_M and assuming a flat universe, we find that the equation of state parameter of the dark energy lies in the range $-1.48 < w < -0.72$ at 95% confidence. If we further assume that $w > -1$, we obtain $w < -0.73$ at 95% confidence. These constraints are similar in precision and in value to recent results reported using the *WMAP* satellite, also in combination with the 2dF Redshift Survey.

Subject headings: cosmological parameters — cosmology: observations — distance scale — galaxies: distances and redshifts — supernovae: general

On-line material: machine-readable tables

[1] Based in part on observations with the NASA/ESA *Hubble Space Telescope,* obtained at the Space Telescope Science Institute, which is operated by the Association of Universities for Research in Astronomy (AURA), Inc., under NASA contract NAS 5-26555. This research is primarily associated with proposal GO-8177, but also uses and reports results from proposals GO-7505, 7588, 8641, and 9118.

[2] CFHT: Based in part on observations taken with the Canada-France-Hawaii Telescope, operated by the National Research Council of Canada, le Centre National de la Recherche Scientifique de France, and the University of Hawaii. CTIO: Based in part on observations taken at the Cerro Tololo Inter-American Observatory. Keck: Some of the data presented herein were obtained at the W. M. Keck Observatory, which is operated as a scientific partnership among the California Institute of Technology, the University of California, and the National Aeronautics and Space Administration. The Observatory was made possible by the generous financial support of the W. M. Keck Foundation. UH: Based in part on observations with the University of Hawaii 2.2 m telescope at Mauna Kea Observatory, Institute for Astronomy, University of Hawaii. UKIRT: Based in part on observations with the United Kingdom Infrared Telescope (UKIRT) operated by the Joint Astronomy Centre on behalf of the UK. Particle Physics and Astronomy Research Council. VLT: Based in part on observations obtained at the European Southern Observatory, Paranal, Chile, under programs ESO 64.O-0391 and ESO 64.O-0404. WIYN: Based in part on observations taken at the WIYN Observatory, a joint facility of the University of Wisconsin–Madison, Indiana University, Yale University, and the National Optical Astronomy Observatories.

[3] Institute for Astronomy, University of Hawaii, 2680 Woodlawn Drive, Honolulu, HI 96822; jt@ifa.hawaii.edu, barris@ifa.hawaii.edu.

[4] The Research School of Astronomy and Astrophysics, The Australian National University, Mount Stromlo and Siding Spring Observatories, via Cotter Road, Weston Creek PO 2611, Australia; brian@mso.anu.edu.au.

[5] Cerro Tololo Inter-American Observatory, Casilla 603, La Serena, Chile; nsuntzeff@noao.edu, kkrisciunas@noao.edu, pcandia@ctiosz.ctio.noao.edu.

[6] Harvard-Smithsonian Center for Astrophysics, 60 Garden Street, Cambridge, MA 02138; kirshner@cfa.harvard.edu, pchallis@cfa.harvard.edu, tmatheson@cfa.harvard.edu.

[7] Departamento de Astronomía y Astrofísica, Pontificia Universidad Católica de Chile, Casilla 306, Santiago 22, Chile; aclocchi@astro.puc.cl.

[8] Department of Astronomy, 601 Campbell Hall, University of California, Berkeley, CA 94720-3411; alex@astro.berkeley.edu, weidong@astro.berkeley.edu, acoil@astro.berkeley.edu, sjha@astro.berkeley.edu.

[9] Department of Physics, University of Notre Dame, 225 Nieuwland Science Hall, Notre Dame, IN 46556-5670; pgarnavi@miranda.phys.nd.edu, sholland@nd.edu.

[10] Department of Astronomy, University of Washington, Box 351580, Seattle, WA 98195-1580; hogan@astro.washington.edu, stubbs@astro.washington.edu.

[11] Las Campanas Observatory, Casilla 601, La Serena, Chile; mmp@lco.cl.

[12] European Southern Observatory, Karl-Schwarzschild-Strasse 2, Garching, D-85748, Germany; bleibund@eso.org, jspyromi@eso.org.

[13] Space Telescope Science Institute, 3700 San Martin Drive, Baltimore, MD 21218; ariess@stsci.edu.

[14] Stockholm Observatory, SCFAB, SE-106 91 Stockholm, Sweden; jesper@astro.su.se.

[15] Deceased 2001 December 12.

1. INTRODUCTION

1.1. *SNe Ia and the Accelerating Universe*

Discovering Type Ia supernovae (SNe Ia) with the intent of measuring the history of cosmic expansion began in the 1980s with pioneering efforts by Nørgaard-Nielsen et al. (1989). Their techniques, extended by the Supernova Cosmology Project (Perlmutter et al. 1995) and by the High-z Supernova Search Team (HZT; Schmidt et al. 1998), started to produce interesting results once large-format CCDs were introduced on fast telescopes. Efforts to improve the use of SNe Ia as standard candles by Phillips (1993), Hamuy et al. (1995), and Riess, Press, & Kirshner (1996) meant that data from a modest number of these objects at $z \approx 0.5$ should produce a significant measurement of cosmic deceleration. Early results by Perlmutter et al. (1997) favored a large deceleration, which they attributed to Ω_M near 1. But subsequent analysis of an augmented sample (Perlmutter et al. 1998) and independent work by the HZT (Garnavich et al. 1998a) showed that the deceleration was small, and far from consistent with $\Omega_M = 1$.

Both groups expanded their samples and both reached the surprising conclusion that cosmic expansion is accelerating (Riess et al. 1998a; Perlmutter et al. 1999). Cosmic acceleration requires the presence of a large, hitherto undetected component of the universe with negative pressure: the signature of a cosmological constant or other form of "dark energy." If this inference is correct, it points to a major gap in current understanding of the fundamental physics of gravity (e.g., Carroll 2001,[16] Padmanabhan 2002). The consequences of these astronomical observations for theoretical physics are important and have led to a large body of work related to the cosmological constant and its variants. For astronomers, this wide interest creates the obligation to test and repeat each step of this investigation that concludes that an unexplained energy is the principal component of the universe.

Formally, the statistical confidence in cosmic acceleration is high—the inference of dark energy is not likely to result simply from random statistical fluctuations. But systematic effects that change with cosmic epoch could masquerade as acceleration (Drell, Loredo, & Wasserman 2000; Rowan-Robinson 2002). In this paper we not only provide a statistically independent sample of well-measured supernovae, but through the design of the search and execution of the follow-up, we expand the redshift range of supernova measurements to the region $z \approx 1$. This increase in redshift range is important because plausible systematic effects that depend on cosmic epoch, such as the age of the stellar population, the ambient chemical abundances, and the path length through a hypothesized intergalactic absorption (Rana 1979, 1980; Aguirre 1999a, 1999b) would all increase with redshift. But, for plausible values of Ω_Λ and Ω_M, 0.7 and 0.3 for example, the matter-dominated deceleration era would lie just beyond $z = 1$. As a result, the *sign* of the observed effect on luminosity distance would change: at $z \approx 0.5$ supernovae are *dimmer* relative to an empty universe because of recent cosmic acceleration, but at $z \approx 1$ the integrated cosmological effect diminishes, while systematic effects are expected to be larger (Schmidt et al. 1998).

[16] Carroll (2001) available at: http://www.livingreviews.org/Articles/Volume4/2001-1carroll.

Confidence that the universe is dominated by dark energy has been boosted by recent observations of the power spectrum of fluctuations in the cosmic microwave background (de Bernardis et al. 2002; Spergel et al. 2003). Since the CMB observations strongly favor $\Omega_{\rm tot} = 1$ to high precision (± 0.02), and direct measurements of Ω_M from galaxy clusters seem to lie around 0.3 (Peacock et al. 2001), mere subtraction shows there is a need for significant dark energy that is not clustered with galaxies. However, this argument should not be used as an excuse to avoid scrutiny of each step in the supernova analysis. Supernovae provide the *only* qualitative signature of the acceleration itself, through the relation of luminosity distance with redshift, and most of that effect is produced in the recent past, from $z = 1$ to the present, and not at redshift 1100 where the imprint on the CMB is formed. This is why more supernova data, better supernova data, and supernova data over a wider redshift range are needed to confirm cosmic acceleration. This paper is a step in that direction.

The most likely contaminants of the cosmological signal from SNe Ia are luminosity evolution, gray intergalactic dust, gravitational lensing, or selection biases (see Riess 2000; Filippenko & Riess 2001; Leibundgut 2001 for reviews). These have the potential to cause an apparent dimming of high-redshift SNe Ia that could mimic the effects of dark energy. But each of these effects would also leave clues that we can detect. By searching for and limiting the additional observable effects we can find out whether these potential problems are important.

If luminosity evolution somehow made high-redshift SNe Ia intrinsically dimmer than their local counterparts, supernova spectra, colors, rise times and light-curve shapes should show some concomitant effects that result from the different velocities, temperatures, and abundances of the ejecta. Comparison of spectra between low-redshift and high-redshift SNe Ia (Coil et al. 2000) yields no significant difference, but the precision is low and the predictions from theory (Höflich, Wheeler, & Thielemann 1998) are not easily translated into a limit on possible variations in luminosity. Some troubling differences in the intrinsic colors of the high- and low-redshift samples have been pointed out by Falco et al. (1999) and Leibundgut (2001). Larger, well-observed samples, including the one reported here, will show whether this effect is real.

Gray dust that absorbs without producing as much reddening as Galactic dust could dim high-redshift SNe Ia without leaving a measurable imprint on the observed colors. Riess et al. (1998a) argued that dust of this sort would need to dim distant supernovae by 0.25 mag at $z \approx 0.5$ in a matter-only universe. To produce the dimming we attribute to acceleration, dust would also increase the variance of the apparent SN Ia luminosities more than is observed. However, such dust, if smoothly dispersed between the galaxies, could appear degenerate with cosmic acceleration (Rana 1979, 1980; Aguirre 1999a, 1999b). Aguirre's electromagnetic calculations of the scattering properties for intergalactic dust show that it can produce less reddening than Galactic dust, but it cannot be perfectly gray. Near-infrared observations of one SN Ia at ≈ 0.5 (Riess et al. 2000) do not show the presence of this form of dust. Further observations over a wide wavelength range have been obtained by our team to construct a more stringent limit; these will be reported in a future paper (S. Jha et al. 2003b, in preparation). Recent work by Paerels et al. (2002), which failed to

detect X-ray scattering off gray dust around a $z = 4.3$ quasar, seems to indicate that gray, smoothly distributed, intergalactic dust has a density that is too low by a factor of 10 to account for the 0.25 mag dimming seen in the SN Ia Hubble diagram.

Selection biases could alter the cosmological inferences derived from SNe Ia if the properties of distant supernovae are systematically different from those of the supernovae selected nearby. Simple luminosity bias is minor because the scatter in supernova luminosities, after correction for the light-curve shape, is so small (Schmidt et al. 1998; Perlmutter et al. 1999; Riess et al. 1998a). However, the nearby sample of SNe Ia currently spans a larger range of extinctions and intrinsic luminosities than has been probed for SNe Ia at $z \approx 0.5$. Most searches to date have only selected the tip of the iceberg: most supernovae at high redshift lie below the sensitivity limit. We assume that we are drawing from the same population as nearby, but it would be prudent to test this rigorously. To make the SN evidence for dark energy robust against sample selection effects, we need more sensitive searches for SNe Ia at $z \approx 0.5$ that could detect intrinsically dim or extinguished SNe Ia so we can verify that the distant supernovae have a similar range of extinctions and intrinsic luminosities as the nearby sample. This was one goal of the 1999 search reported here.

Extending the data set to higher redshift is a more ambitious and difficult way to test for the cosmological origin of the observed dimming effect. Evolution or dust would most naturally lead to increased dimming at higher redshift, while cosmic deceleration in the early matter-dominated era ($z \geq 1.2$) would imprint the opposite sign on luminosity distances. A search at higher redshift demands that we search to fainter flux limits in bands that are shifted to the red to detect rest-frame B and V. In this paper, we describe a sensitive search in the R and I bands carried out at the Canada-France-Hawaii Telescope (CFHT) and at the Cerro Tololo Inter-American Observatory (CTIO) in 1999. For the highest redshifts, we detect flux emitted in the ultraviolet at the source. Members of the HZT have also embarked on an extensive study of the U-band properties of nearby supernovae that will help with the interpretation of these high-redshift objects (S. Jha, A. G. Riess, & R. P. Kirshner 2003a, in preparation).

Performing these tests requires searching for SNe Ia with a deeper magnitude limit in redder bands than previous searches. This approach can sample the full range of extinctions and luminosities at $z \approx 0.5$ and test for a turn-down in the Hubble diagram at $z \geq 1$. Thus far, direct measurement of deceleration at early epochs rests in observations of one SN Ia, SN 1997ff, at the remarkably high redshift of $\sim$1.7. These observations match best with a dark-energy source for the observed behavior of SNe Ia (Riess et al. 2001). But this single object represents just one data point isolated from the body of SN Ia observations—and there is evidence that this object could be significantly magnified by gravitational lensing (Benítez et al. 2002). A continuous sample from $z \approx 0.5$ through $z \approx 1$ out to $z \geq 1.5$ is required to make this crucial test convincing. The present paper represents a step in that direction by extending the sample to $z \approx 1$. Future discoveries of very high z supernovae using the Advanced Camera for Surveys on the *Hubble Space Telescope* (*HST*), successfully installed in 2002, will help bridge the gap from the high-redshift end.

Section 2 of this paper describes the search, shows spectra of the supernovae, and provides our photometric results. Section 3 gives an account of the analysis including K-corrections, fits to the light curves, and luminosity distances. In § 4 we discuss the inferred cosmological parameters, and in § 5 we discuss how these results can be used to test for systematic errors in assessing cosmic acceleration from SN Ia observations. Some novel features of the analysis are described more thoroughly in the Appendix.

2. OBSERVATIONS

2.1. *Search*

The SNe Ia reported here were discovered at the CFHT using the CFH 12K camera and at the CTIO 4 m Blanco telescope using the CTIO Mosaic camera. The CFH 12K camera provides 0.″206 pixels and a field of view of 0.33 deg^2, and the CTIO mosaic has 0.″270 pixels with a field of view of 0.38 deg^2.

We obtained templates in 1999 October and obtained subsequent images in November to find new objects, plausibly supernovae, with a rise time in the observer frame of $\sim$1 month. On the nights of 1999 October 3 and October 7 (UT dates are used throughout this paper), we obtained CFH 12K images of 15 fields (5 deg^2) in the I and R bands with median seeing of 0.″65 and 0.″72, respectively. We integrated for a total of 60 minutes on six of the I-band fields and three of the R-band fields, and 30 minutes on the rest. Each integration was of 10 minutes duration, with the frames dithered by small offsets to help in removing cosmic rays and CCD defects. The photometric zero points were approximately $I = 35.0$ and $R = 35.6$ mag for the 60 minute exposures—in other words, a source of that magnitude would produce 1 e^-. This permits detection of stars with $m = 24$ mag at a signal-to-noise ratio (S/N) of 12 and 16, respectively, or detection of a supernova with $m = 24$ mag at a S/N of 9 and 11 in a difference search. A first-epoch search scheduled in October at CTIO was clouded out.

Despite a generous time allocation, we ran into difficulties at CFHT a month later because of weather. The first night (1999 November 2) had clouds and bad seeing (>1″). We accumulated 60 minutes in the I band for each of eight fields, but only one of these fields contributed to the search, yielding one SN Ia: SN 1999ff. The second night (1999 November 3) had a mean extinction of about 0.5 mag from clouds, but the seeing was very good (median 0.″59). We obtained reasonably good data in the I band for eight fields, with integrations of 60 minutes for five of these, and 30 minutes for three. Three nights later (1999 November 6) we searched at CTIO, using R-band observations from CFHT as the first-epoch observations. Although the CTIO data enabled us to confirm the SN Ia found in the I band at CFHT, and produced several candidates that required spectroscopic follow-up, we found no new supernovae from these observations. Spectra of several CTIO candidates revealed the disappointing fact that our attempt to compare November CTIO observations with October CFHT templates produced subtly false candidates where a mismatch between the CFHT and CTIO filters caused the difference between the two to give the illusion of a new objects appearing between October and November. In fact, these were M stars or emission-line galaxies whose Hα emission line fell at the red end of the R-band filter. Only the comparison of

TABLE 1
FALL 1999 OBSERVATIONS

SN Name	R.A. (J2000)	Decl. (J2000)	$E(B-V)$	N_{obs}	MJD_{max}	Nickname
SN 1999fw	23 31 53.03	+00 09 32.3	0.039	25	51482	Nell
SN 1999fh	02 27 58.33	+00 39 36.8	0.031	15	51488	Fearless Leader
SN 1999ff	02 33 54.39	+00 32 55.6	0.026	25	51494	Bashful
SN 1999fn	04 14 03.88	+04 17 55.0	0.326	46	51498	Scooby Doo
SN 1999fj	02 28 23.72	+00 39 09.6	0.030	20	51475	Natasha
SN 1999fm	02 30 35.62	+01 09 43.3	0.023	21	51488	Fred
SN 1999fk	02 28 53.88	+01 16 24.2	0.030	22	51492	Velma
SN 1999fv	23 30 35.80	+00 16 40.0	0.041	8	51457	Dudley Doright
SN 1999fo	04 14 45.75	+06 38 34.3	0.291	11	...	Gertie
SN 1999fi	02 28 11.67	+00 43 39.3	0.031	12	...	Boris
SN 1999fu	23 29 48.21	+00 08 27.0	0.048	11	...	Alvin

CFHT data with CFHT templates provided genuine detections of supernovae.

Our reduction and search procedure, detailed by Schmidt et al. (1998), consists of bias subtraction, flat-fielding, subtraction of *I*-band fringes, masking bad columns, and finally combining dithered images to reject cosmic rays and moving objects. In each field, we identified stars, performed an astrometric solution, and then remapped the image onto a common coordinate system. (This mapping is flux conserving but uses a Jacobian to restore the photometric accuracy that is destroyed by flat-fielding.) For each pair of images of a field, from the first (October) and second (November) epoch, we then used the algorithms described by Alard & Lupton (1998) to convolve the image with the better seeing into agreement with the worse image. Next we matched the flux levels and subtracted.

These difference images were then searched automatically for residuals resembling the point-spread function (PSF), with possible SNe Ia flagged for further inspection by humans. Simultaneously, we searched all image pairs by inspecting the difference images by eye. We found little difference in the detection efficiency between the semiautomatic approach and inspection by experienced observers. For all the SN Ia candidates, we inspected each of the individual exposures to ensure that the putative SN Ia was not a cosmic ray, moving object, or CCD flaw. All 37 final candidates were tabulated along with estimated *I* and *R* magnitudes (from the CTIO observations), including the properties of the possible host galaxy and distance from the center of the host. This candidate list became our observing list for subsequent spectroscopic investigation.

Different exposure times in different fields, variable extinction due to clouds, changes in seeing, and sensitivity variations among the chips in the CFH 12K mosaic make it hard to quantify a single detection threshold for genuine events in this search. We believe that, overall, our search is 95% effective for objects brighter than $I = 23.5$ mag, and substantially better than 50% at $I = 24$ mag. In some favorable cases we found objects as faint as $I = 24.5$ mag.

We began observing our 37 candidate objects at the Keck II telescope on 1999 November 8. Our aim was to determine the nature of each object and to measure its redshift. Of these 37, two turned out to be active galactic nuclei at redshifts of 1.47 and 1.67; one was an M star and two were galaxies with Hα emission admitted because of mismatched *R* filters; five had disappeared, suggesting either that the discovery was well past maximum or the detection was spurious; four were judged to be Type II supernovae from spectra or blue color; two were too bright to be of interest for our purposes, $I \approx 21$ mag in bright host galaxies, possibly nearby SNe II, for which we did not spend time to get spectra; three were SNe Ia with $0.3 < z < 0.7$ which we chose not to follow; seven were faint candidates for which we did not have time to get spectra; and 11 were the candidate SNe Ia which we chose to follow. These are shown in Figure 1. The selection of objects was based on color information (we chose objects with colors consistent with SNe Ia with any amount of reddening, in the range $0.1 < z < 1.5$); the amount of variation of the SN, with preference given to objects that were not seen in the previous epoch, but that had varied significantly; the host galaxy brightness at the supernova position, avoiding supernova candidates on extremely bright backgrounds; and host brightness/size—avoiding supernovae in low-redshift galaxies ($z < 0.1$). These selection effects are all undesirable, but with limited telescope time, they were necessary compromises to achieve the goals of the search.

Table 1 lists the J2000 coordinates of the SNe Ia, the Galactic extinction from Schlegel, Finkbeiner, & Davis (1998), the number of photometric observations in various bandpasses accumulated from various telescopes, the modified Julian date of maximum light, and our nickname for the supernova, assigned before there was a designation for each event in the IAU Circulars (see Tonry et al. 1999). The last three objects on the list are real objects which we pursued, but based on our spectra and subsequent light curves, the evidence is too weak to consider them SNe Ia. SN 1999fi (Boris) was very close to SN 1999fj, so it did not cost extra observing time to get photometry, but the other two (SN 1999fo and SN 1999fu) fooled us into making 22 photometric observations and expending many hours of Keck time to get spectra that were, in the end, inconclusive. Although these two are real events, with a definite flux increase from October to November and a decrease in flux after November, we have not shown that they are SNe Ia, and they are not included in the analysis.

2.2. *Spectral Observations and Reductions*

We obtained spectra of our SN Ia candidates with LRIS (Oke et al. 1995) on the Keck II telescope during five nights between 1999 November 8 and 14. The seeing varied from $0\farcs8$ to $1\farcs1$ during the first three nights and was $\sim 0\farcs5$ on the last two nights. We used a $1\farcs0$ slit for all of our

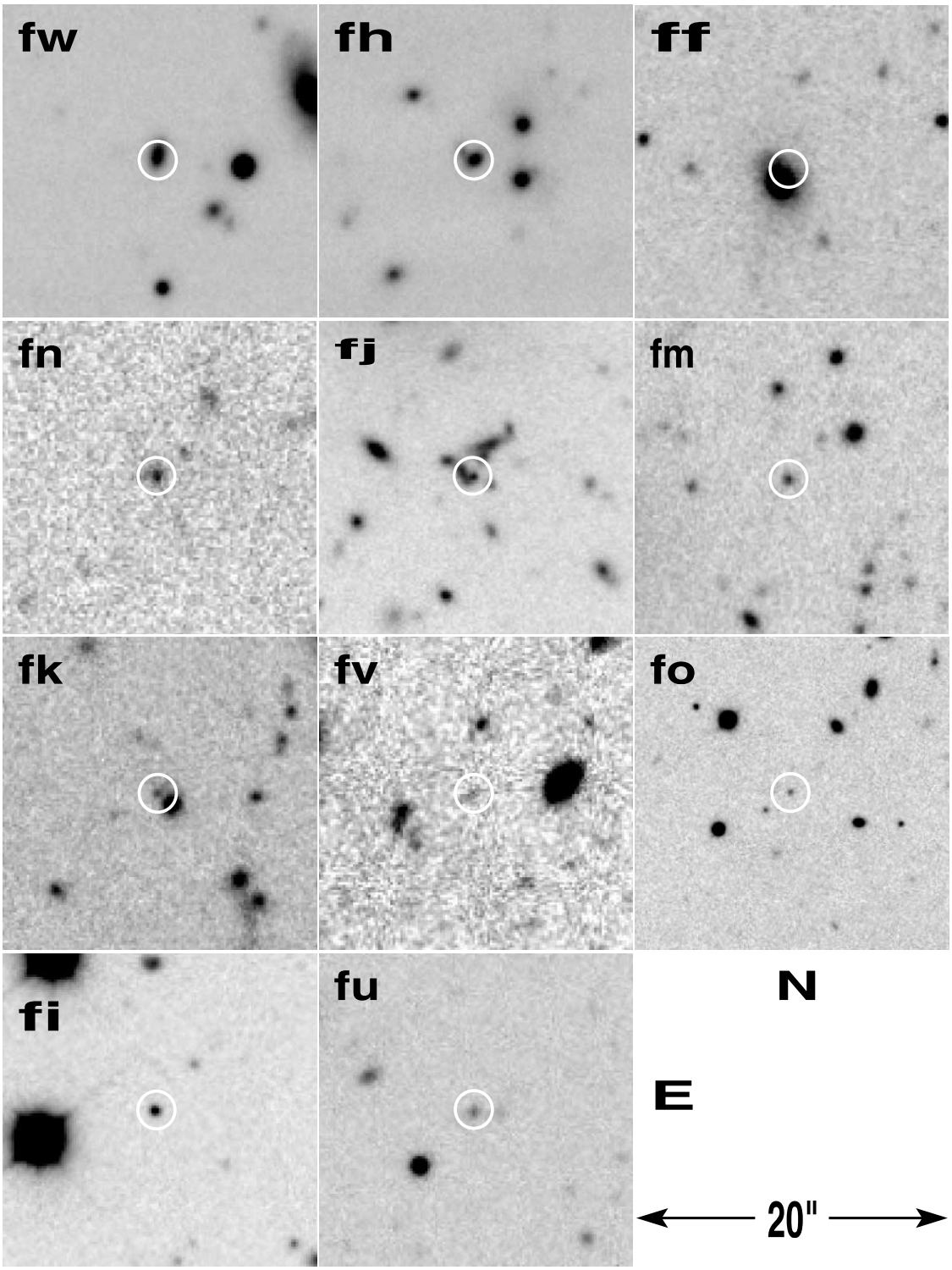

FIG. 1.—Host galaxies for the 11 supernovae. Each image is 20″ on a side and taken from an average of several I-band frames. A 2″ radius circle marks the position of the supernova. North is at the top and east to the left in each image.

observations, except for SN 1999fv, where we used a 0.″7 slit on one night. We used a 150 line mm^{-1} grating for the first half of the run, then switched to a 400 line mm^{-1} grating for the second half in order to better remove night-sky lines. The resulting spectral resolution is ~20 Å for the 150 line mm^{-1} grating and ~8 Å for the 400 line mm^{-1} grating. The pixel size for the 150 and 400 line mm^{-1} gratings is ~5 and ~2 Å pixel^{-1}, respectively. The total exposure times for each SN Ia are listed in Table 2. We moved the object along the slit between integrations to reduce the effects of fringing. The slit was oriented either near the parallactic angle, or to include the nucleus of the host galaxy or a nearby bright star

TABLE 2
FALL 1999 SPECTROSCOPIC DATA

SN Name	z	Type	Number of Nights	Exposure (s)	z Determination
SN 1999fw	0.278	Ia	1	1200	broad SN features
SN 1999fh	0.369	Ia	1	1800	[O II] λ3727 in SN spectrum
SN 1999ff	0.455	Ia	1	2200	Balmer lines in galaxy spectrum
SN 1999fn	0.477	Ia	2	5900	[O II] λ3727 in SN spectrum
SN 1999fj	0.816	Ia	1	3600	[O II] λ3727 in SN spectrum
SN 1999fm	0.95	Ia?	2	6600	broad SN features
SN 1999fk	1.057	Ia?	2	7000	[O II] λ3727 in SN spectrum
SN 1999fv	1.17–1.22	Ia	2	10000	broad SN features
SN 1999fo	1.07	?	3	14200	Ca H and K dip in spectrum
SN 1999fi	1.10	?	1	5000	[O II] λ3727 in spectrum
SN 1999fu	1.135	?	2	7200	[O II] λ3727 in spectrum

to provide quantifiable astrometry along the slit and to define the trace of a source along the spectral direction.

When using the 150 line mm^{-1} grating, internal flat-field exposures and standard stars were observed both with and without an order-blocking filter to remove contamination from second-order light. For the high-z SN Ia observations no order-blocking filter was needed, as there is very little light from the object or from the sky below an observed wavelength of 4000 Å. We used BD $+17^{\circ}4708$ as a standard star for the first two nights and Feige 34 (Massey et al. 1988) for the last three nights. Standard CCD processing and optimal spectral extraction were done with IRAF.[17] We used our own IDL routines to calibrate the wavelengths and fluxes of the spectra and to correct for telluric absorption bands. For SNe Ia that were observed on more than one night, the data were binned to the larger pixel size if different gratings were used, scaled to a common flux level, and combined with weights depending on the exposure time to form a single spectrum.

2.3. *SNe Ia Spectra and Redshifts*

The SNe Ia spectra are shown in Figure 2 at their observed wavelengths. For each SN Ia we list in Table 2 the redshift, the supernova type, the number of nights observed with Keck, the total exposure time, and an explanation of how the redshift was derived. For SNe Ia with narrow emission or absorption lines from the host galaxy light, we determined the redshift by using the centroid of the line(s) with a Gaussian fit. For the three SN Ia spectra without narrow lines from the host galaxy, we use the broad SN Ia features to determine the redshift by cross-correlating the high-z spectrum with low-z SN Ia spectra obtained near maximum light. We also include galaxy and M star spectra among our templates for cross-correlation with spectra without narrow emission lines. Errors on the redshifts are ± 0.001 ($1\,\sigma$) when based on a narrow line and ± 0.01 when based on broad SN Ia features. The redshift of SN 1999fv has a large uncertainty (1.17–1.22) due to the low S/N of the spectrum (see Coil et al. 2000 for further discussion).

[17] IRAF is distributed by the National Optical Astronomy Observatory, which is operated by the Association of Universities for Research in Astronomy, Inc., under cooperative agreement with the National Science Foundation.

Figure 3 presents the high-z spectra smoothed with a Savitsky-Golay filter of width 100 Å, sorted by redshift, with the lowest z SN Ia at the top. This polynomial smoothing filter preserves line features better than boxcar smoothing, which damps out peaks and valleys in a spectrum. The width of the smoothing filter is apparent in the [O II] λ3727 emission line seen in many of the spectra. We also plot two low-z SNe Ia (SN 1989B, Wells et al. 1994; SN 1992A, Kirshner et al. 1993) and a low-z SN Ic [SN 1994I dereddened by $E(B-V) = 0.45$ mag; Filippenko et al. 1995] for comparison, all with ages before or at maximum light. Features which distinguish a SN Ia (Filippenko 1997) are deep Ca II H and K absorption near 3750 Å, the Si II λ4130 dip blueshifted to 4000 Å, and Fe II λ4555 and/or Mg II λ4481, the combination of which create a distinct double-bump feature centered at 4000 Å. For the lower z spectra we have enough wavelength coverage to see 6150 Å, where the Si II λ6355 absorption feature is prominent in SNe Ia, but beyond $z \approx 0.4$ this feature becomes difficult to detect. Early SN Ic spectra look similar to SNe Ia blueward of 5000 Å, but lack the prominent Si II dip at 4000 Å which leads to the double-bump feature seen only in SNe Ia.

SN 1999fw, 1999fh, 1999ff, 1999fn, and 1999fj are all clearly SNe Ia. SN 1999fm is a Type I SN, but we cannot distinguish from the spectrum alone whether it is a Type Ia or Ic. SN 1999fk shows a definite rise around 4000 Å and has some hints of a double peak at this location, but is not definitively a SN Ia. SN 1999fv shows some bumps centered at 4000 Å, which, as discussed in Coil et al. (2000), are plausibly SN Ia features at a redshift of $\sim$1.2. All eight of these supernovae are used in this paper.

SN 1999fi, 1999fu, and 1999fo do not show any SN features in their spectra. For each of these systems, we have a redshift; for SN 1999fi and 1999fu this comes from a single line we assume to be [O II] λ3727. For SN 1999fo the spectrum appears to have Ca II H and K absorption at $z = 1.07$. As stated above, these three objects are not used in the analysis.

2.4. *Properties of the Host Galaxies*

Host galaxies and the environment around each supernova are shown in Figure 1. The images are the average of the *I*-band images with the best seeing. No host was detected for SN 1999fm. SN 1999fj appears in a small group of galaxies, and its host is assumed to be the elongated galaxy just east of the supernova. Host magnitudes were measured

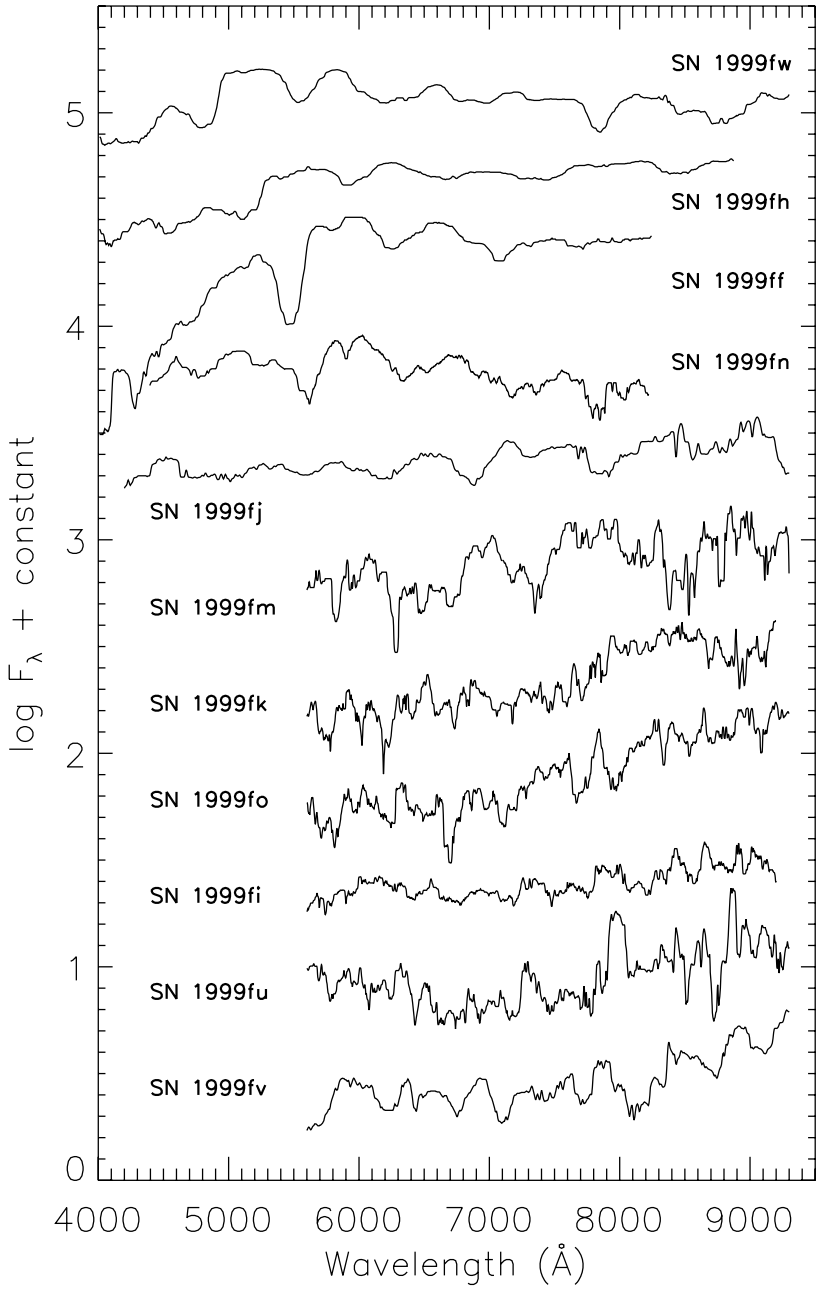

FIG. 2.—High-z supernova spectra at their observed wavelengths, smoothed by a 32 pixel running median and a Gaussian of 4 pixel σ

from images taken after the supernova had faded. For the brightest hosts, the flux was summed out to an isophote of 26 mag arcsec^{-2}, but for the faint hosts the flux was summed in a 4″ diameter aperture. The results, without correction for extinction, are given in Table 3 .

Offsets between the supernovae and their hosts are also given in Table 3, as is the projected separation in kpc assuming a flat Λ-dominated cosmology with $\Omega_M = 0.3$. The distribution of projected separations for these new supernovae is narrower than that of earlier searches (Farrah et al. 2002), meaning that our supernovae were discovered closer to the hosts. This may be due to the greater depth of this search and better image quality as it attempted to detect objects at $z > 1$.

2.5. *Photometric Calibrations and Reductions*

The photometric data gathered of the supernovae discovered at CFHT and CTIO came from a wide variety of instruments and telescopes, including Keck LRIS, Keck ESI, Keck NIRC, VLT FORS, VLT ISAAC, UKIRT UFTI, UH 2.2 m, VATT, WIYN, and *HST*. We accumulated a total of 216 observations of our 11 candidate SNe Ia over the span of approximately one year, in the V, R, I, Z, and J bandpasses, totaling ~200 hr of exposure time. The seeing of the combined, remapped images had a median of 0.″83, with quartiles at 0.″72 and 1.″04.

Calibration of these data turned out to be especially challenging, as a result of a variety of difficulties. The

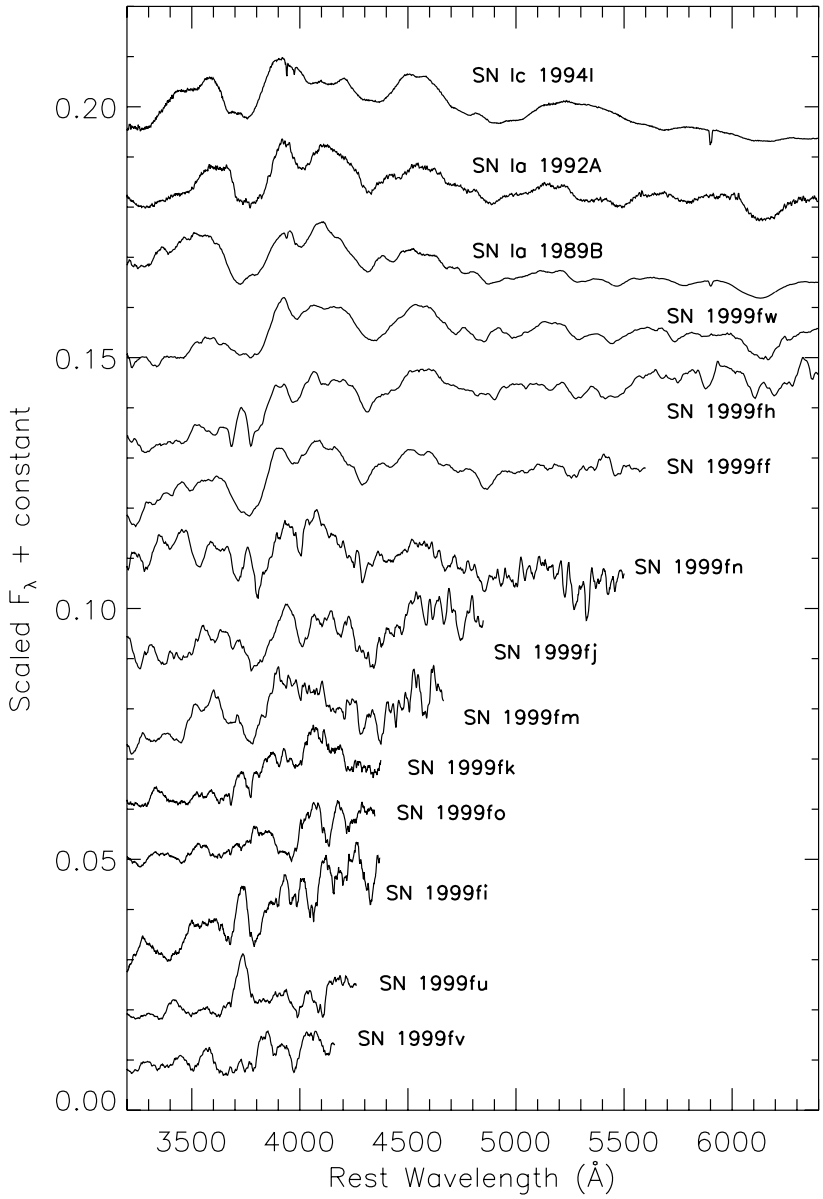

FIG. 3.—High-z SN spectra, shifted to rest wavelengths, smoothed by a Savitsky-Golay filter with a width of 100 Å and compared to two low-z SNe Ia (SN 1992A and SN 1989B) and a low-z SN Ic (SN 1994I). The high-z SN spectra are shown sorted by redshift, with the lowest z SN at the top. Based on these spectra, we cannot conclude that SN 1999fi, 1999fo, and 1999fu are SNe Ia.

photometric calibration of stellar sequences near our SNe Ia was intended to come from observations with the UH 2.2 m and the CTIO 1.5 m telescopes. To this end, we observed Landolt (1992) standards in V, R, I, and Z on a variety of photometric nights, and also observed our SN Ia fields to establish the magnitudes of local photometric reference stars. We took a sequence of short exposures of a constant flat-field to establish the shutter timing error, and checked the linearity of the CCD by exposures of different duration. For standard-star reductions we summed the flux (with background subtraction) of each star through a 14″ aperture, and calculated an atmospheric extinction term for each night. A typical scatter in this fit to air mass and color was 0.02 mag, and arises from the usual causes: sky errors, imperfect flat-fielding, changes in atmospheric transparency, CCD nonlinearity, shutter timing errors, and PSF or scattered-light variations. In the case of the UH 2.2 m data, there were some observations which deviated significantly from the root mean square (rms) error of the majority of data. This was eventually tracked down to an error in dome control, causing observations to be vignetted by the dome shutter. The UH 2.2 m data are therefore not completely reliable photometric calibrations. The CTIO 1.5 m data had no such problems, and were taken on absolutely photometric nights. However, they do not cover all fields, and the overlap in brightness between data with high photometric accuracy from the 1.5 m and the unsaturated data from the larger telescopes was not large.

To bridge these calibration difficulties, we combined two additional calibration sources, the Sloan Digital Sky Survey (SDSS; Stoughton et al. 2002) and the 2001 HZT campaign

TABLE 3
FALL 1999 HOST GALAXIES

SN Name	Host R	Host I	Host Z	Offset (arcsec)	Projected Separation (kpc)
SN 1999fw	21.1	20.4	...	0.51	2.3
SN 1999fh	21.2	20.8	20.5	0.03	0.2
SN 1999ff	19.9	19.2	19.1	2.01	12.6
SN 1999fn	24.5	23.5	...	0.31	2.0
SN 1999fj	23.3	22.3	21.9	0.89	7.2
SN 1999fm	...	>24.5	...	...	...
SN 1999fk	...	21.9	23.7	1.36	11.9
SN 1999fv	> 26.0	25.8	...	0.30	2.7
SN 1999fo	...	23.1	23.2	0.19	1.7
SN 1999fi	24.8	23.1	22.9	0.16	1.4
SN 1999fu	24.2	23.6	23.5	0.35	3.1

NOTE.—The offset is the angular separation between the SN and host. SN 1999fm had no detectable host. Ellipsis indicate no image available in that band.

(Barris et al. 2002). The 2001 HZT campaign took great pains to obtain very high accuracy photometry at the CTIO 1.5 m telescope, which was reduced in a manner identical to the 1999 CTIO data, as described above. These observations of more than 200 stars were used to calibrate a catalog of R, I, and Z photometry of about 4000 stars near $\alpha = 02^{\rm h}28^{\rm m}$, $\delta = +00^\circ35'$, derived from CFHT+12K mosaic images. The R and I bandpasses of these data were transformed to the standard Kron-Cousins system (Kron & Smith 1951; Cousins 1976), using the CTIO derived values, and the Z band was transformed to the CTIO system, as described below.

This 2001 HZT catalog and all of our supernovae at R.A. = $23^{\rm h}$ and $02^{\rm h}$ are encompassed by the SDSS catalog. Using the matched stars at $02^{\rm h}$ between our 2001 HZT photometric catalog and the SDSS (using PSF-derived magnitudes of the Sloan data—not the default available on the Web site), we derived the following transformations from the SDSS g', r', i', and z' magnitudes and our Vega-based magnitudes:

$$V - g' = +0.172 - 0.745(g' - r') ,$$
$$R - r' = -0.122 - 0.316(r' - i') ,$$
$$I - i' = -0.423 - 0.378(i' - z') ,$$
$$Z - z' = -0.511 - 0.037(r' - i') ,$$
$$Z - z' = -0.508 - 0.267(r' - i') + 0.424(i' - z') .$$

The two-color fit to $Z - z'$ is slightly better, but obscures the fact that Z and z' are nearly identical, apart from a zero-point offset.

For all colors, the scatter in the transformation for individual stars (which are not dominated by shot noise like the faint SDSS stars, or by saturation like the CFHT stars of roughly the same magnitude) is approximately 0.02 mag rms. These transformations enable us to calibrate the R, I, and Z 1999 CFHT survey fields via the SDSS early-release data.

Since we did not observe in the V band during our fall 2001 campaign, we needed extra steps to derive the calibration of the V observations for our 1999 data. We used Landolt (1992) stars in our fields and derived a satisfactory relation for $0 < (R - I) < 1$ mag,

$$(V - R) = -0.024 + 1.104(R - I) .$$

For redder stars, there are significant differences in the V-band colors for giants and dwarfs, which we sought to avoid. This relation allowed us to produce "V" magnitudes for the fall 2001 catalog, using the R and I magnitudes. We then compared the stars that were also available from SDSS, and derived a g' to V transformation. While individual stars can have substantial errors via these transformations, in the mean of hundreds of stars that we used these transformations are better than 0.01 mag.

The Z band was both important and problematic for us. At $z > 1$, the rest-frame B band starts to shift beyond the observer's I band, and the systematics of rest-frame U-band observations were not yet well established at the time of these observations (but see S. Jha et al. 2003a, in preparation), so we needed a color for our SNe Ia based on bandpasses redder than I. There is a variety of Z bands; ours is a Vega-normalized bandpass defined by the CTIO natural system (RG850, two aluminum reflections, atmosphere, and a SITe CCD red cutoff), and it is quite well described as a sum of two Gaussians, one centered at 8800 Å with a σ of 280 Å and a height of 0.86, and the other at 9520 Å with a σ of 480 Å and a height of 0.41. The Z bandpass and this approximation are illustrated in Figure 4. Our Z-band observations were calibrated by observing a series of Landolt stars, whose magnitudes were derived by integrating their spectrophotometry (N. Suntzeff 2003, in preparation) with this bandpass. This system is defined to have $(V - Z) = 0$ mag for Vega.

The SDSS observations covered all our fields except for those containing SN 1999fn and SN 1999fo. For all SNe Ia, except these two, we extracted SDSS stars that fell within the supernova fields, and used the above relations to produce Johnson/Kron-Cousins magnitudes for each star. For SN 1999fn and SN 1999fo, we used our UH 2.2 m photometric observations, verified with a few overlapping stars from the 1999 CTIO 1.5 m observations, to set the R and I magnitudes of a stellar sequence around the SN. The V and Z magnitudes were set using color relations derived above. As stated above, these transformations, while good in the

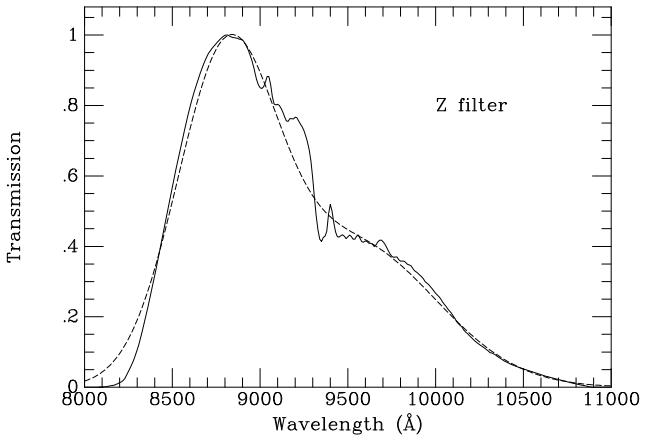

FIG. 4.—Z bandpass used for these observations. The dashed line is an approximation of the actual transmission, made up of two Gaussians as described in the text.

TABLE 4
Local Standard Stars

SN Name	R.A.	Decl.	V	±	R	±	I	±	Z	±
SN1999fu.....	23 29 46.8	+00 11 11	21.43	0.04	20.25	0.06	18.57	0.03	17.92	0.04
	23 29 46.5	+00 04 45	20.70	0.03	19.69	0.04	18.42	0.03	17.93	0.04
	23 29 45.4	+00 09 08	20.74	0.03	19.77	0.04	18.52	0.03	18.05	0.05
	23 29 41.7	+00 10 18	19.40	0.02	18.87	0.03	18.36	0.03	18.20	0.05
	23 29 41.3	+00 11 08	18.58	0.02	18.46	0.02	18.37	0.03	18.37	0.06
	23 29 37.8	+00 05 06	20.73	0.03	19.80	0.04	18.79	0.04	18.40	0.06
	23 29 37.5	+00 10 26	20.99	0.04	19.94	0.05	18.42	0.03	17.82	0.04
	23 29 35.3	+00 10 06	20.94	0.03	19.87	0.05	18.45	0.03	17.89	0.04
SN1999ff.....	02 34 00.2	+00 34 20	20.03	0.02	18.99	0.03	17.62	0.02	17.08	0.03
	02 33 54.2	+00 29 53	19.37	0.02	18.87	0.03	18.38	0.03	18.21	0.05
	02 33 51.7	+00 29 48	18.71	0.02	17.88	0.02	16.96	0.02	16.62	0.02
	02 33 57.1	+00 31 18	19.90	0.02	19.10	0.03	18.31	0.03	18.02	0.04
	02 33 53.3	+00 28 18	19.71	0.02	18.79	0.03	17.74	0.02	17.33	0.03
	02 33 46.5	+00 27 08	20.85	0.03	19.70	0.04	18.02	0.03	17.36	0.03
	02 33 36.6	+00 28 39	20.02	0.03	19.29	0.03	18.56	0.03	18.30	0.06

Note.—Table 4 is published in its entirety in the electronic edition of the *Astrophysical Journal*. A portion is shown here for guidance regarding its form and content.

mean, may not be appropriate for unusual stars (or quasars), and consequently, our derived magnitudes are based relative to the sequence of stars, rather than weighting any individual star too highly. The adopted standard-star sequences in the vicinity of each supernova are given in Table 4. This calibration procedure is far from ideal, but cross-checks suggest it is as good as the Sloan zero-point uncertainty, 0.04 mag.

We calibrated the *J*-band data from VLT and UKIRT using observations of 10 standard stars from Persson et al. (1998). The Keck data were calibrated by transferring the photometric zero points from the UKIRT observations to a galaxy in the field of SN 1999fn.

All our supernova images were compared with the above stellar sequences to derive zero points. The star fluxes were obtained using the Vista *psf* routine, which sums up the light within a radius of 20 pixels around a star, subtracts a fitted sky value, and rejects contamination from neighboring objects. Comparison of the fluxes and magnitudes, with due regard for saturation and magnitude errors, gave us a flux-magnitude zero point and error for most images. For *HST* images, we used the precepts of Dolphin (2000) to convert fluxes to magnitudes.

2.6. *Photometry of SNe Ia*

Our reductions of deep supernova observations obtained after the candidates were identified are very similar to the reductions carried out during the search. After bias subtraction, flat-fielding, *I*-band and *Z*-band fringe correction, masking bad columns, and combination of dithered images while rejecting cosmic rays and moving objects, we identified stars relative to a fiducial image and performed an astrometric solution. We remapped a 1024×1024 pixel subarray of the source image onto a tangent plane coordinate system with $0\farcs2$ pixels. The *HST* observations had a small enough field of view and large enough distortion that some amount of star selection by hand was necessary to obtain a satisfactory astrometric match.

We had expected to use *HST* to acquire very high quality light curves for a subset of our objects, but the gyro failure in fall 1999 made *HST* unavailable until after this group of SNe Ia had disappeared. We did succeed in using *HST* to get template observations of the host galaxies after the supernovae had faded for most of our targets. Late-time templates are very helpful in subtracting the host galaxy accurately and in setting the SN Ia flux zero point.

Most modern supernova light curves are derived by subtraction of a template image taken before the supernova explosion or long after, so that it carries no supernova flux. While this sets a good flux zero point for the subtraction, it also inflicts a common, systematic flux error on the light curve, which can be substantial if the template observation has poor S/N or very different seeing.

To avoid these correlated errors, we subtracted all $N(N-1)/2$ pairs of observations from one another. We carried this out using the Alard & Lupton (1998) code mentioned previously. This procedure produces negative fluxes for some subtractions, but it has the advantage that *every* observation serves as a template for the entire light curve. The details of this procedure are given in the Appendix. We have found that this procedure reduces the errors by a factor of about $\sqrt{2}$ (Novicki & Tonry 2000).

There are two unresolved questions after the $N(N-1)/2$ procedure has been followed. We do not know a flux zero point, since it has been removed when we difference images, and we need a flux-to-magnitude conversion that incorporates the independent magnitude zero points established for each image.

The flux zero point is generally established by late-time observations when there is no remaining supernova flux. This is an improvement over the usual "template" method, because the flux zero point that comes out of the $N(N-1)/2$ procedure for the late-time point comes from the average comparison with all the other observations, and the relative fluxes of all the other observations do not depend solely on the final observation. In some cases where we had several late-time points without supernova flux, we adjusted the flux zero point to be an average of those points, or to include a first point that was obtained prior to the supernova explosion.

Infrared template images were available only for SN 1999fm and SN 1999fk, so we used standard PSF

TABLE 5
OBSERVATIONS OF THE EIGHT SUPERNOVAE

MJD	m	±	K	±	ObsID
	V		$K_{V\to B}$		
51496.25.....	22.18	0.15	−0.34	0.04	991114_uh
51514.20.....	23.84	0.86	−0.24	0.03	991202_uh
51529.21.....	>24.50	...	−0.21	0.04	991217_uh
51875.25.....	>24.50	...	−0.26	0.05	001127_esi
	R		$K_{R\to V}$		
51455.27.....	>24.50	...	−0.20	0.15	991004_12k
51488.15.....	21.30	0.01	−0.42	0.04	991106_8k
51496.22.....	21.43	0.02	−0.30	0.06	991114_uh
51514.26.....	22.40	0.13	−0.15	0.06	991202_uh
51517.21.....	22.66	0.09	−0.14	0.07	991205_lris
51529.28.....	23.54	0.21	−0.09	0.07	991217_uh

NOTE.—Table 5 is published in its entirety in the electronic edition of the *Astrophysical Journal*. A portion is shown here for guidance regarding its form and content.

photometry with the DAOPHOT II/Allstar package (Stetson 1987; Stetson & Harris 1988) to measure the J-band magnitudes of the SNe corrected to the same aperture used for the standard stars. SN 1999fm was not visible in the J band. SN 1999fk is near the edge of its host, so contamination from the galaxy is negligible. SN 1999fn and SN 1999fv are embedded in their hosts, so contamination may be significant. SN 1999ff is located in a bright ($J \approx 17.5$ mag) elliptical galaxy for which it was essential to subtract the host. We used the IRAF/STSDAS analysis isophote tasks to construct a model of the host, subtracted our model, and then performed PSF photometry on the supernova. We were unable to define a PSF for the Keck observations of SN 1999fn because of the lack of suitable stars in the Keck/NIRC field of view, so we performed aperture photometry in an aperture with a radius of 1″.

Table 5 gives the derived supernova light curves, and Figure 5 shows the data points and typical fitted light curves.

3. SN Ia ANALYSIS

3.1. *K-Corrections*

K-corrections were calculated using the formulas described by Kim, Goobar, & Perlmutter (1996) and Schmidt et al. (1998). The apparent brightness of a supernova observed in filter j, $m_j(t)$, but with a $z = 0$ absolute

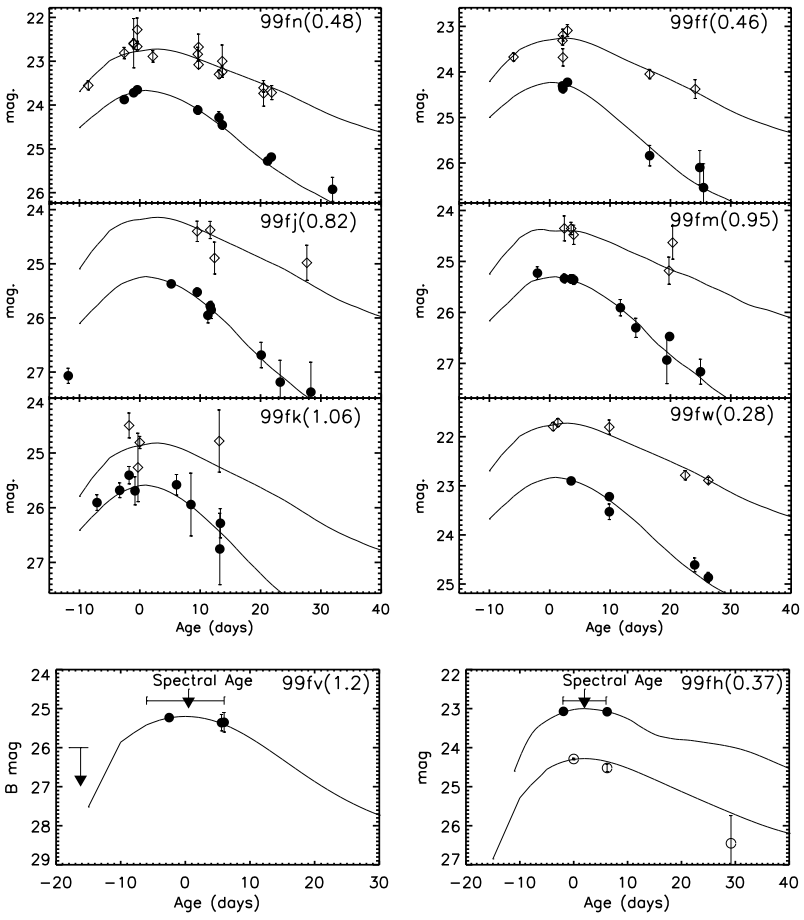

FIG. 5.—MLCS fits to our eight SNe Ia. The open diamonds represent K-corrected V-band fits, while the filled circles represent K-corrected B-band fits, offset by +1 mag, except for SN 1999fh, which is $V + 1$ and R. SN 1999fo, 1999fi, and 1999fu have no light curves because we could not establish from the spectra that these were indeed SNe Ia, so they were not followed. Redshifts are indicated in parentheses.

magnitude light curve in filter i, $M_i(t)$, is given by

$$m_j(t) = M_i((1+z)t') + 25 + 5\log\left(\frac{D_L}{\mathrm{Mpc}}\right) + K_{ij}((1+z)t') ,$$

where K_{ij} is given by

$$K_{ij} = 2.5\log\left[(1+z)\frac{\int F_\lambda(\lambda)S_i(\lambda)d\lambda}{\int F_\lambda(\lambda/(1+z))S_j(\lambda)d\lambda}\right] + \mathscr{Z}_j - \mathscr{Z}_i , \quad (1)$$

for filter energy sensitivity functions S_i and S_j, with zero points $\mathscr{Z}_i$ and $\mathscr{Z}_j$, and supernova spectrum F_λ. The luminosity distance, D_L, depends on the cosmological parameters, and is discussed extensively by Schmidt et al. (1998).

For multifilter light-curve shape (MLCS) fitting, K-corrections were calculated in the same manner as for Riess et al. (1998a), as part of the fitting process, using a prescription similar to that of Nugent et al. (2002). For K-corrections presented in Table 5, we used a set of 135 SN Ia spectra ranging from 14 days before maximum light to 92 days after maximum light. Extending the work of Nugent et al. (2002), before applying the K-correction formulae, the SN Ia spectra of each epoch were matched to the dereddened *UBVRI* color curves of a well-observed set of SN templates, by warping the spectral energy response with a spline containing knots at the effective wavelengths of each filter. In our case we used the compilation of Jha (2002) for SN 1991T, 1994D, 1996X, 1997bp, 1997bq, 1997br, 1998ab, 1998aq, 1998bu, 1998es, 1998V, 1999aa, 1999ac, 1999by, 1999dq, and 1999gp. The spectra were corrected for the estimated host extinction in the rest frame, as well as for Galactic extinction in the observer's frame using the Schlegel et al. (1998) values and the Savage & Mathis (1979) reddening law. The modified spectra were then used to calculate the K-corrections, providing a series of K-correction estimates as a function of SN age, and of SN template type. These values were fitted with a 3 knot spline, and uncertainties estimated from the scatter of allowable templates as dictated by the light-curve fits (in this case, the modified "dm15" method of Germany 2001).

Our K-corrections were used to fit the light curve and update the time of maximum light, as well as the allowable supernova template type and host extinction, and the whole process was iterated until convergence (only two iterations were required). Table 5 lists the derived K-corrections for each observation along with their uncertainties.

3.2. *Light-Curve Fits Using MLCS*

We fit the photometry of the eight SNe Ia shown in Figure 5 using either the MLCS algorithm as described by Riess et al. (1998a) or Riess et al. (2001), depending on the quality of the data.

For SNe Ia whose light curve constrains the time of maximum well and whose colors provide sufficient leverage on potential reddening, we fit the photometry using the MLCS algorithm as described by Riess et al. (1998a). This method employs the observed correlation between light-curve shape, luminosity, and colors of SNe Ia in the Hubble flow, leading to significant improvements in the precision of distance estimates derived from SNe Ia (Hamuy et al. 1995, 1996a; Riess, Press, & Kirshner 1995, 1996).

The empirical model for a SN Ia light and color curve is described by four parameters: a date of maximum (t), a luminosity difference (at maximum, Δ), an apparent distance modulus (μ_B), and an extinction (A_B). Due to the redshifts of the supernova host galaxies, we first correct the supernova light curves for Galactic extinction (Schlegel et al. 1998), and then determined the host-galaxy extinction.

Although the best extinction estimates and most precise distances are found from SN Ia light curves that have extended temporal and spectral coverage, ideally to $\sim$100 days after maximum and 4 or 5 bandpasses (Jha 2002), we only use data within 40 days of maximum light and in rest-frame B and V to match the data that can be sampled at high redshift. This should only compromise our accuracy slightly, however.

For SN 1999fv and SN 1999fh, failure of the *HST* gyros led to data with less than optimal coverage in time. For these two objects we used the snapshot distance method (Riess et al. 1998b), which employs the observed SN Ia spectrum to constrain the age. This approach is significantly less precise than the distance from a well-sampled light curve.

3.3. *Light Curve Fits Using $\Delta m_{15}(B)$ and dm15*

We also use the Δm_{15} method of Phillips et al. (1999) to estimate a distance to each of our SN Ia. Originally, the method characterized the light curve by a parameter tied to the B-band photometry: the decline in magnitudes for a SN Ia in the first 15 days after B-band maximum. With the accumulation of a larger number of well-sampled light curves, it became possible to expand the method so that $\Delta m_{15}(B)$ is determined from the B, V, and I-band light curves. The Phillips et al. method then compares the light curve of a new object with a small number (six) of template light curves.[18]

In contrast to the MLCS method of Riess et al. (1996, 1998a), the Δm_{15} method does not produce a *continuum* of "synthetic" templates. Rather, there are a small number of *discrete* templates. The reddening of a SN Ia is determined from the $B-V$ and $V-I$ colors at maximum, and from the $B-V$ colors between 30 and 90 days after V-band maximum. It is assumed that unreddened SNe Ia of all decline rates show uniform late-time color curves, as found by Lira (1995). Jha (2002, § 3) found that the "Lira law" holds well for the 44 SNe Ia studied by him. Only exceptional cases like SN 2000cx seem to deviate greatly from the relation (Li et al. 2001b; Candia et al. 2003).

Distances using the modified dm15 method are described in detail by Germany (2001). In summary, well-observed SNe Ia (approximately 15 objects) are fitted with a spline in *BVRI* and assigned a value of $\Delta m_{15}(B)$ based on the method of Phillips (1993) and Phillips et al. (1999). These templates are extended to explosion times using the rise-time measurements of Riess et al. (1999b). SNe Ia at $cz > 4000$ km s^{-1} with extinction values from Phillips et al. (1999) are fitted with these templates, with the best-fitting template used to assign these objects a dm15 value and maximum light values $B_{\max}$, $V_{\max}$, $R_{\max}$, and $I_{\max}$. The Hubble velocity then provides an absolute magnitude in each band, from which M_{BVRI} versus dm15 relationships are derived. The values found from these relationships are applied to the set of well-observed templates to create a set of absolute magnitude

[18] The six templates are based on the light curves of seven objects: SN 1991T, 1991bg, 1992A, 1992al, 1992bc, and 1992bo+1993H. The method now compares the light curve of a new object with six template light curves (Hamuy et al. 1996a).

light curves in *BVRI*. To measure the distance to a new supernova, each template is fitted to the data, marginalizing over time of maximum and A_V, to find the distance modulus of the object. The distance is then estimated as the χ^2-weighted average of each template distance, with the distance uncertainty derived from the union of all templates and distances that have acceptable χ^2 fits.

3.4. *Light Curve Fits Using BATM*

The Bayesian Adapted Template Match (BATM) Method, described by J. L. Tonry (2003, in preparation), uses a set of approximately 20 nearby supernova light curves that are well observed in multiple colors and that span the range of absolute luminosity to predict what they would look like at an arbitrary redshift with an arbitrary host extinction through the actual filters used for observation. Since these SNe Ia do not in general have a significant amount of spectrophotometry, the BATM method uses approximately 100 spectral energy distributions (SEDs) of other SNe Ia at a variety of SN Ia ages, and warps the SEDs into agreement with the photometry. Given each of the template predictions and a light curve of a new SN Ia, the BATM method then calculates the likelihood distribution as a function of explosion time t_0, host extinction A_V, and distance d, and marginalizes over t_0 to get a likelihood as a function of A_V and d. This is multiplied by a prior for A_V, which is a Gaussian of $\sigma = 0.2$ mag for negative A_V, a Gaussian of $\sigma = 1.0$ for positive A_V, and a delta function at $A_V = 0$ of equal weight. Unfortunately, for these observations (and probably most extant high-redshift SN Ia distances) there is strong covariance between d and A_V, and the choice of prior makes a nonnegligible difference in the final estimate for d. The BATM method then combines the probability distributions for all of the template SNe Ia and marginalizes over A_V to get a final estimate for the distance.

The BATM method is still undergoing improvement and is not currently "tuned" to minimize scatter of the SNe Ia in the Hubble flow. For example, one might expect that certain bandpasses or time spans during a supernova's light curve might be better predictors of distance (the MLCS method is designed to optimize those choices). The BATM method simply fits all the data available in the observed bandpasses (avoiding the use of *K*-corrections) without regard to how a set of SNe Ia in the nearby Hubble flow behave. As a result, the scatter of the BATM method for these Hubble-flow SNe Ia is somewhat larger than that of MLCS (0.22 mag vs. 0.18 mag), but it has a different, and perhaps smaller, set of systematic errors.

3.5. *Fall 1999 Distances*

We list the distance estimates and uncertainties based on our light curves from MLCS, $\Delta m_{15}(B)$, dm15, and BATM in Table 6, along with the empty universe distance modulus corresponding to each redshift. The uncertainties are formal error estimates derived from each method, and we do not attempt here to evaluate whether these estimates are accurate. Below, in Table 8, we do pay attention to the self consistency of the various error estimates. This assumes a nominal value of $H_0 = 65$ km s^{-1} Mpc^{-1}, although the cosmological inferences do not generally depend on the value of H_0. The estimates are generally consistent with each other, and we list a "final" distance that is the median of the estimates of each of the four methods. The uncertainty of this "final" distance is taken to be the median of the errors of the contributing methods, because we regard the process of taking a median of different analysis methods not so much as sharpening our precision as rejecting non-Gaussian results.

3.6. *Rates*

From observations of just three SNe Ia at $z \approx 0.4$, Pain et al. (1996) calculated a rate of SNe Ia that amounts to 34 SNe Ia yr^{-1} deg^{-2}, with a 1 σ uncertainty of a factor of $\sim$2, for objects found in the range of $21.3 < R < 22.3$ mag. A more recent estimate by Pain et al. (2002) is $(1.53 \pm 0.3) \times 10^{-4}\ h^3$ Mpc^{-3} yr^{-1} at a mean redshift of 0.55. Cappellaro, Evans, & Turatto (1999) report a nearby rate of SNe Ia of $0.36 \pm 0.11\ h^2$ SNU (where 1 SNU $\equiv 10^{10}\ L_{B_\odot}$ per century) or $(0.79 \pm 0.24) \times 10^{-4}\ h^3$ Mpc^{-3} yr^{-1}, using a local luminosity density of $\rho = 2.2 \times 10^8\ h\ L_{B_\odot}$ pc^{-3}. [There is significant uncertainty in the luminosity density, however: Marzke et al. (1998) obtained 1.7×10^8, and Folkes et al. (1999) found 2.7×10^8.] Pain et al. (2002) report a very modest increase in the rate of SNe Ia with redshift, perhaps tracking the star formation rate, which Wilson et al. (2002) estimate as being proportional to $(1 + z)^{1.7}$ in a flat universe with $\Omega_M = 0.3$.

Although our fall 1999 observing was focused on finding candidates for detailed study, it still contains useful information on supernova rates. Two facts help establish rates from this search. First, our observations were very deep in the *I* band (since we were primarily searching for $z > 1$ SNe Ia), and second, because we also sought to find good $z \approx 0.5$ SNe Ia for *HST* observations, we obtained spectra for every plausible candidate SN Ia with $z < 0.7$. While we did not obtain light curves for all these candidates, we do know which were Type Ia, and we know their redshifts. This

TABLE 6
DISTANCE MODULI ($h = 0.65$)

SN Name	MLCS	Δm_{15}	dm15	BATM	Final	$\Omega = 0$
SN 1999fw	40.97 ± 0.31	40.89 ± 0.15	40.80 ± 0.24	40.99 ± 0.42	40.93 ± 0.27	40.82
SN 1999fh	...	...	41.77 ± 0.26	41.46 ± 0.47	41.61 ± 0.36	41.52
SN 1999ff	42.38 ± 0.29	42.60 ± 0.22	42.35 ± 0.43	42.61 ± 0.32	42.49 ± 0.30	42.05
SN 1999fn	42.69 ± 0.26	42.36 ± 0.16	41.98 ± 0.40	42.19 ± 0.23	42.27 ± 0.24	42.18
SN 1999fj	44.03 ± 0.22	43.59 ± 0.37	43.76 ± 0.35	43.55 ± 0.43	43.67 ± 0.36	43.62
SN 1999fm	44.18 ± 0.22	44.06 ± 0.23	43.84 ± 0.37	43.77 ± 0.35	43.95 ± 0.29	44.05
SN 1999fk	$<44.23 \pm 0.30$	...	44.26 ± 0.39	44.17 ± 0.36	44.23 ± 0.37	44.36
SN 1999fv	$<44.59 \pm 0.39$	...	...	$<44.19 \pm 0.45$	$<44.39 \pm 0.42$	44.74

TABLE 7
PEAK MAGNITUDES OF NORMAL SNE IA

z	B	V	R	I	Z	J
0.05.....	17.37	17.41	17.36	17.82	17.72	(17.70)
0.10.....	18.94	18.88	18.80	19.20	19.24	(19.30)
0.20.....	(20.70)	20.29	20.27	20.36	20.75	(20.96)
0.30.....	(21.94)	21.08	21.07	20.97	21.28	(21.63)
0.40.....	(23.07)	21.89	21.62	21.55	21.67	21.97
0.50.....	(24.06)	(22.59)	22.10	22.01	21.96	22.35
0.60.....	(24.90)	(23.26)	22.59	22.41	22.37	22.79
0.70.....	(25.53)	(23.97)	23.06	22.70	22.70	23.06
0.80.....	(26.00)	(24.75)	(23.54)	22.91	23.01	23.11
0.90.....	(26.39)	(25.46)	(24.06)	23.12	23.17	23.20
1.00.....	(26.75)	(26.03)	(24.61)	23.48	23.39	23.25
1.10.....	(27.08)	(26.45)	(25.14)	23.78	23.50	23.38
1.20.....	(27.39)	(26.78)	(25.66)	(24.19)	23.72	23.59
1.30.....	(27.67)	(27.07)	(26.13)	(24.59)	24.11	23.72
1.40.....	(27.95)	(27.35)	(26.55)	(24.91)	(24.39)	23.94
1.50.....	(28.20)	(27.60)	(26.93)	(25.36)	(24.70)	24.08
1.60.....	(28.45)	(27.85)	(27.24)	(25.85)	(25.04)	24.18
1.70.....	(28.68)	(28.08)	(27.51)	(26.30)	(25.32)	24.32
1.80.....	(28.90)	(28.30)	(27.75)	(26.77)	(25.72)	24.38

provides the raw material for a computation of the supernova rate.

At the outset we need to make some reasonable assumption about the underlying luminosity distribution of SNe Ia, calculate what fraction of these we would see in our search, and then derive the supernova rate. We assume a luminosity function for SNe Ia at maximum that consists of three Gaussians: 64% "normal" SNe Ia with mean absolute magnitude $M_B = -19.5$ mag [$h \equiv H_0/(100 \text{ km s}^{-1} \text{ Mpc}^{-1}) = 0.65$] and dispersion $\sigma = 0.45$ mag, 20% "SN 1991T" SNe Ia with $M_B = -19.8$ mag and dispersion $\sigma = 0.30$ mag, and 16% "SN 1991bg" SNe Ia with $M_B = -18.0$ mag and dispersion $\sigma = 0.50$ mag (Li et al. 2001a).

Table 7 gives values that a "normal" SN Ia might achieve at maximum, derived from the colors of SN 1995D at maximum and the spectral energy distribution of SN 1994S, with parentheses indicating magnitudes that are less accurate because they involve an extrapolation beyond the data for either of these two objects.

We work in a space of redshift z and $m_{\max}$, where m is the bandpass of interest (I band here). We use the magnitudes of SN 1995D at maximum and the spectral energy distribution (SED) of SN 1994S to convert a point in this space to a value for the B-band (rest-frame) maximum and therefore a density from our luminosity function. We multiply in a volume factor $dV/dz/d\Omega$ and a factor of $(1+z)^{-1}$ because we are interested in the observer's rate of observing SNe Ia. All of this is done for a flat universe with $(\Omega_M, \Omega_\Lambda) = (0.3, 0.7)$. We then convolve the resulting distribution with a dust extinction distribution which approximates the detailed curves of Hatano, Branch, & Deaton (1998): 25% of hosts are "bulge systems" with the probability of a given host A_B given by $f(A_B) \propto 0.02\delta(A_B) + 10^{-1.25-A_B}$, and 75% of hosts are "disk systems" with probability $f(A_B) \propto 0.02\delta(A_B) + e^{-3.77-A_B^2}$. (The redshifted SEDs tell us how the observed I-band extinction depends on a given host galaxy extinction A_B.) This gives us a distribution for the observed rate of SNe Ia as a function of peak apparent I-band magnitude.

However, two complications arise. The "observation time" that must be multiplied into this distribution is a convolution of the search time and the intrinsic time that a given SN Ia is above the detection threshold. Also, our supernova detection threshold is not based only on peak I-band magnitude. We have two search epochs, separated by 31 days, and we have a sensitivity of $I \approx 24$ mag to the flux *difference* between the first and second epochs.

Using the formalism of the BATM method, we place SN 1995D ($\Delta m_{15} = 0.99$, MLCS $\Delta = -0.42$) and SN 1999by ($\Delta m_{15} = 1.93$, MLCS $\Delta = +1.48$) in the z-$m_{\max}$ space. Any point in the space between them is assigned a light curve which is the flux interpolation between the redshifted light curves of SN 1995D and SN 1999by. Points that lie brighter or fainter than these two SNe Ia are assigned copies of one or the other light curves, which are simply scaled brighter or fainter to match the desired peak brightness. Given a light curve, we calculate the visibility time for each point in the (z, m_I) diagram, using a 31 day lag time and a sensitivity of $I < 24$ mag. (Our actual probability of detecting a supernova rolls off gradually at fainter magnitudes, but we had S/N ≈ 10 at $I < 24$ mag and we ignored candidates we thought would peak at $I > 24$ mag, hence the approximation of a step at $I = 24$ mag.)

The resulting difference light curve is identical to the actual light curve when the explosion occurs after the first epoch, but for explosions that erupted earlier than the first epoch, taking the difference between our two observation epochs decreases the difference and can be negative. Low-luminosity SNe Ia with rapid rise and declines would be visible for a shorter time than higher luminosity SNe Ia with their slowly declining light curves, so they are less likely to be found. For the purpose of calculating rates, the total time that a supernova could be detected is a convolution of the time that the difference flux from the supernova explosion exceeds the sensitivity limit and the search time (a delta function in this case).

Figure 6 shows contours of predicted rates (number per observer's month per square degree per magnitude per unit redshift). We plot our eight SNe Ia as well as three other SNe Ia that we did not follow. Without light curves for these three, we can only show the discovery (difference) magnitude, which is an upper limit to the peak I-band magnitude that was eventually reached.

The normalization of Figure 6 is adjusted to bring the cumulative distribution as a function of z into agreement with our observations. Figure 7 integrates the lower panel of Figure 6 over magnitude and then assembles the cumulative predicted number of SNe Ia as a function of redshift. We compare this with the number observed to normalize the model. Our sensitivity limit was approximately $I < 24$ mag, and the time between our first and second search epochs was 31 days. Our total area surveyed (including the cloudy second epoch) was 3.0 deg^2, of which we lost about 15% through chip edges, bad columns, stars, etc., so our effective search area was about 2.5 deg^2. Subsequent tests of our search technique using synthetic SNe Ia injected into the images indicate that we miss very few objects down to the quoted sensitivity limit.

Uncertainties in the searched area, effective time sampling, and modeling of supernova properties amount to perhaps 10%–20%, and a similar uncertainty is the fraction of objects that we detected photometrically but for which we did not obtain spectroscopy. Since our goal was to find

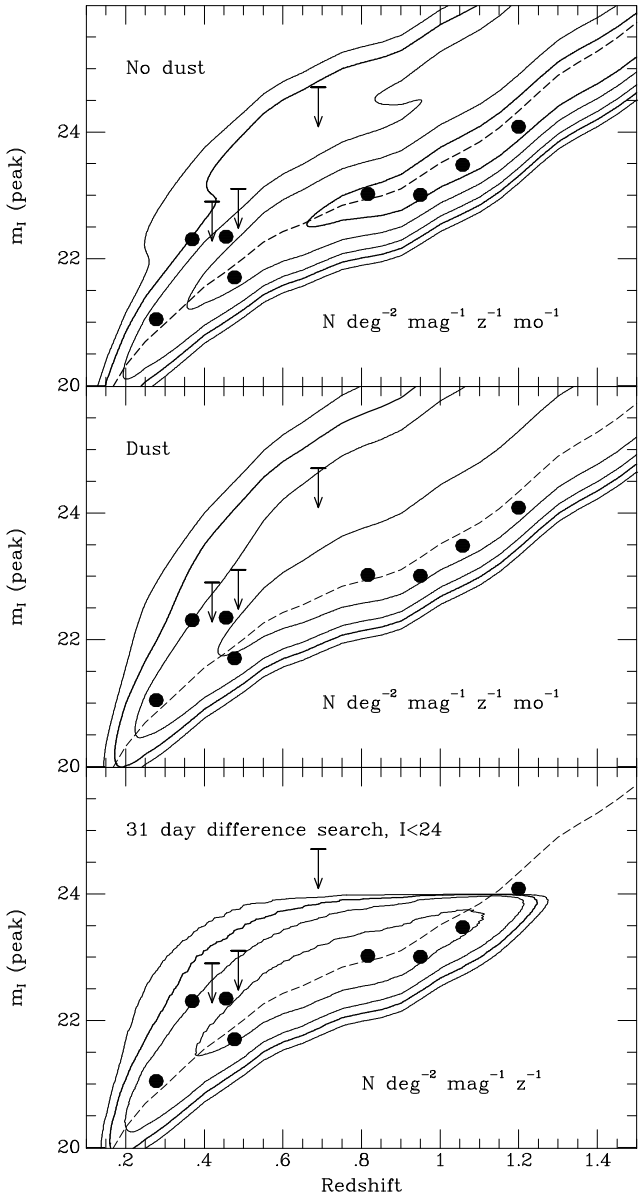

FIG. 6.—Distribution of SNe Ia occurrence as a function of peak I-band magnitude and redshift. Contours of predicted rates are drawn with heavy curves at 1 and 10, and light curves at intervening intervals of 2 and 5. The ridge line of an unreddened "normal" SN Ia is shown by a dashed line. The upper panel shows the distribution based on the SN Ia luminosity function if there were no reddening; the middle panel shows the effect of convolving with the model extinction distribution; and the bottom panel shows the expected distribution for our search parameters.

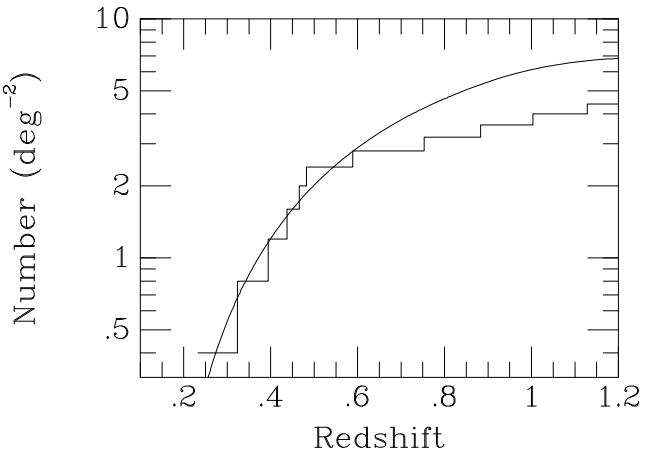

FIG. 7.—Cumulative number of SNe Ia discovery as a function of redshift. The histogram is the observed SNe Ia; the curve is the prediction of what we should have seen given a flux limit of $I < 24$ mag and a 31 day difference search. We think that our search is nearly complete for $z \leq 0.6$, but do *not* claim completeness for $z > 0.6$, because of the necessity to pick a subset for spectroscopy.

suitable targets for *HST* studies and to find supernovae at $z \approx 0.5$, we were not complete in our spectroscopic follow-up. Subjective factors go into the decision of which objects to follow. For example, if we find a candidate at $I = 23.5$ mag, but it appears to be in a galaxy at $z \approx 0.3$, we might very well choose not to get a spectrum, reasoning that "the supernova is well past maximum" or "it might be a Type II" or "it might be highly extinguished, or a SN 1991bg-type." Spectroscopic resources are *so* valuable that our first priority, to obtain targets, often outweighs our desire to control systematics. The factors in these decisions change with redshift of the supernova: we believe we were complete in our search to $z < 0.6$ (even though we did not follow three SNe Ia photometrically), but we were definitely not complete for more distant and fainter SNe Ia. The bottom panel of Figure 6 shows that the counts of SNe Ia to a redshift of $z < 0.6$ are not very sensitive to our estimate of our completeness limit.

Figure 7 shows the comparison between this model cumulative distribution and the observed rates for our fall 1999 campaign. The Poisson statistics of the eight SNe Ia counted with $z < 0.6$ are still the largest source of uncertainty, and we estimate that our overall normalization is accurate to about 35%. The slope agreement between the observations and the model in Figure 7 reassures us that our model is reasonably accurate.

These model predictions, which we calculate for comparison with the observations, include complicated factors for visibility within a time window and sensitivity limit, convolution with dust extinction, time dilation factors of $(1 + z)$, and volume factors of $dV/dz/d\Omega$. The fundamental normalization that goes into the calculation and that brings the model into agreement with the observations shown in Figure 7 amounts to 40,000 SNe Ia of all subtypes per Gpc^3 per (rest-frame) year for the Hubble constant used above ($H_0 = 65$ km s^{-1} Mpc^{-1}) for the SN Ia luminosity function. Put in more sensible units, this is a rate of $r = (1.4 \pm 0.5) \times 10^{-4}\ h^3$ Mpc^{-3} yr^{-1} SNe Ia at a mean redshift of $z = 0.46$. So the observed rate of SNe Ia from a shell at redshift z is

$$dN = r\, d\Omega (dV/dz/d\Omega)(1 + z)^{-1} \Delta t\ ,$$

where Δt has to be integrated over the luminosity function of SNe Ia and the search parameters.

These rates are in excellent agreement with those of Pain et al. (2002), and are not inconsistent with the local rates from Cappellaro et al. (1999), particularly given the uncertainty in the local luminosity density.

Although we were not complete in our counts of SNe Ia at $z \approx 1$, we do not believe it is possible that the rate of SNe Ia closely tracks the star formation rate (SFR). Application

of the SFR from Wilson et al. (2002) would suggest that the rate at $z \approx 1.1$ should be 3 times as great as occurs locally and nearly twice as great as the rate at $z = 0.46$. Our model illustrated in Figure 7, if altered from a constant rate per comoving volume to one that tracks the SFR of Wilson et al. (2002), would predict 16 SNe Ia deg^{-2} in our search instead of 6.5 (we discovered 4). It is our impression that the constant rate per volume is closer to the truth—SNe Ia at $m_I = 24$ mag are simply not that common. Obviously, SN Ia explosions lag star formation by some unknown time distribution. This suggests that the lag must span a substantial fraction of the time between the peak of star formation and the time when a supernova observed at $z \sim 1$ explodes, which is about 2 Gyr. As pointed out by Pain et al. (2002), we should obtain better constraints on any increase in the SN Ia rate at $z > 1$ from ongoing search campaigns.

3.7. *A Homogeneous Set of SN Ia Distances*

As standardizable candles, SNe Ia have played an extremely important role in recent years. However, observations of SNe Ia are so difficult and resource-intensive that the results have appeared in a large number of papers, using a variety of distance zero points, photometric calibrations, etc. We have therefore undertaken to draw all the results available to us together into a single table with a common calibration.

The most recent data apart from the observations presented here are the results from the campaigns of the HZT in 1997 (B. Leibundgut et al. 2003, in preparation), 1998 (N. Suntzeff et al. 2003, in preparation), 1999 (A. Clocchiatti et al. 2003, in preparation), and 2000 (S. Jha et al. 2003a, in preparation).

In the 1997 data, there are four spectroscopically classified SNe Ia (SN 1997as, 1997bb, 1997bh, and 1997bj) and one object in an elliptical galaxy (SN 1997bd) at redshifts in the range 0.33–0.67. The redshifts are all from narrow emission lines associated with the host galaxies, and on the prominent Ca II H and K absorption in the elliptical galaxy. The supernova spectrum in all cases yielded an age concordant with the light curves. Light curves in the *R* and *I* filters have been established for all objects. The campaign in 1997 made use of ground-based telescopes only. The distance moduli, colors, and absorptions are given in Table 8.

From our 1998 campaign, N. Suntzeff et al. (2003, in preparation) report photometry and spectroscopy of six SNe Ia: 1998I, 1998J, 1998M, 1998ac, 1998ai, and 1998aj. A seventh object (SN 1998ah) was only observed spectroscopically. These seven objects range in redshift from 0.43 to 0.887. One of the significant results of the 1998 and 1999 (see below) campaigns was the comparison of the photometry of the SNe Ia and nearby field stars from ground-based and *HST* observations: we found that the zero points of the photometry agree to within 0.02 mag, which is reassuring. Since the highest weighted points in light curves of high-*z* supernovae are usually the *HST* data, owing to their smaller statistical uncertainties, we naturally wanted to compare photometry obtained on the ground and in space. Because the evidence from supernova observations for a nonzero cosmological constant hinges on a systematic faintness of SNe Ia at $z \approx 0.5$ by 0.22 mag, we are now quite confident that the systematic faintness of supernovae at such redshifts is *not* due to a zero-point error between space-based and ground-based light curves.

In the spring 1999 campaign, A. Clocchiatti et al. (in preparation) found five spectroscopically classified SNe Ia: SN 1999M, 1999N, 1999Q, 1999S, and 1999U. All of them were followed up from ground-based observatories and two of them, SN 1999Q and SN 1999U, were observed with *HST*. We report in Table 8 the distance moduli to the latter two based on the *HST* photometry. The redshift of SN 1999U was obtained from emission lines in the parent galaxy, and that of SN 1999Q from cross-correlating its spectrum with nearby SN Ia close to maximum light.

The 2000 campaign was intended primarily to investigate the possibility that gray dust was causing the dimming we attribute to cosmology. S. Jha et al. (2003a, in preparation) present photometry over a very wide wavelength range. There are six SNe Ia at a redshift of $\sim$0.5 whose distances

TABLE 8
SN Ia Summary

SN	*l*	*b*	*z*	Host	Reference	log(*cz*)	$\langle \log(dH_0) \rangle$	±	$\langle A_V \rangle$	Contributing
sn72E.....	314.840	30.080	0.0023	N5253	16	2.839	2.399	0.033	0.10	RT
sn80N	240.161	−56.689	0.0056	N1316	9	3.225	3.140	0.043	0.21	RT
sn81B.....	292.970	64.743	0.0072	N4536	2	3.334	3.077	0.041	0.25	RT
sn81D	240.161	−56.689	0.0056	N1316	9	3.225	3.044	0.055	0.31	JT
sn86G	309.543	19.401	0.0027	N5128	26	2.908	2.440	0.035	0.49	RT
sn88U	8.737	−81.227	0.3100	Anon	24	4.968	5.096	0.072	0.10	RT
sn89B.....	241.991	64.403	0.0036	N3627	37	3.033	2.844	0.030	0.74	RST
sn90N	294.369	75.987	0.0044	N4639	21	3.120	3.204	0.035	0.30	RST
sn90O	37.654	28.360	0.0307	M+034403	10	3.964	3.977	0.025	0.09	RPJST
sn90T.....	341.503	−31.526	0.0400	P63925	10	4.079	4.101	0.042	0.25	RJT

NOTE.—Table 8 is published in its entirety in the electronic edition of the *Astrophysical Journal*. A portion is shown here for guidance regarding its form and content.

REFERENCES.—(1) A. Riess et al. 2004, in preparation; (2) Buta & Turner 1983, Tsvetkov 1982; (3) A. Clocchiatti et al. 2003, in preparation; (4) Filippenko et al. 1992, Leibundgut et al. 1993, Turatto et al. 1996; (5) Ford et al. 1993; (6) Garnavich et al. 2001; (7) Germany 2001; (8) Germany et al. 2003; (9) Hamuy et al. 1991; (10) Hamuy et al. 1996b; (11) Jha 2002; (12) Jha et al. 1999, Suntzeff et al. 1999; (13) S. Jha et al. 2003c, in preparation; (14) Krisciunas 2001; (15) Krisciunas et al. 2000; (16) Leibundgut et al. 1991; (17) B. Leibundgut et al. 2003, in preparation; (18) Li et al. 1999; (19) Li et al. 2001b; (20) W. D. Li et al. 2003, in preparation; (21) Lira et al. 1998; (22) Mandel et al. 2001; (23) Modjaz et al. 2001; (24) Norgaard-Nielsen et al. 1989; (25) Perlmutter et al. 1999; (26) Phillips et al. 1999; (27) Richmond et al. 1995, Patat et al. 1996, Meikle et al. 1996; (28) Riess et al. 1998a; (29) Riess et al. 1998b; (30) Riess et al. 1999a; (31) Riess et al. 2000; (32) Riess et al. 2001; (33) N. B. Suntzeff 2001, private communication; (34) N. B. Suntzeff et al. 2003, in preparation; (35) this paper; (36) Turatto et al. 1998; (37) Wells et al. 1994.

we include in Table 8: SN 2000dz, 2000ea, 2000ec, 2000ee, 2000eg, and 2000eh.

In addition to these observing campaigns of the HZT, we also drew from the literature all SN Ia results we could find. Where we had access to the observational data and photometry, we recomputed fits to the distance and extinction using the MLCS98 method of Riess et al. (1998a), the MLCS2k2 improvement of S. Jha et al. (2003a, in preparation), and the dm15 and BATM methods described above. In other cases, such as the Supernova Cosmology Project (SCP; Perlmutter et al. 1999), which has not published their photometry, we took their published distances, extinctions, and uncertainties at face value. One might expect that applying multiple fitting techniques as we have done would help decrease errors in the derived distances. The SCP-only results appear to have at least a factor of 2 more scatter with respect to a cosmological fit than our data. This could be due to the quality of the underlying photometry, or to a less varied approach to the analysis.

Assembling all of these results from the literature and performing new fits when possible, we obtain long lists of SN Ia results for each method that are internally self-consistent, but have unknown offsets with respect to one another because of differing and inconsistent assumptions about Hubble constants and zero points. We also have one more distance measure, derived from the redshift of the SNe Ia in the "Hubble flow" (defined as $0.01 < z < 0.1$) and the luminosity distance for an empty universe,

$$D_L = \frac{cz}{H_0}\left(1 + \frac{z}{2}\right) . \quad (2)$$

All of the methods overlap for many SNe Ia, particularly the Calán-Tololo sample (Hamuy et al. 1996a), with even the SCP results having 17 or 18 overlaps with the rest, and the other methods having 52–108 overlaps. In order to determine the zero-point offsets we compute the median difference between all pairs of methods, forming an antisymmetric matrix, and then fit this matrix as differences between components of a zero-point vector. The residuals are quite well behaved, with the worst agreement between SCP and MLCS98 at 0.07 mag, and the rest 0.02 mag or better. We put all the methods on the Hubble flow zero point, i.e., distance in Mpc multiplied by H_0.

It is beyond the scope of this paper to analyze and optimize the combination of the published data. We do note that there actually does appear to be a modest improvement in accuracy (judged by scatter with respect to the cosmological line) by combining different fitting methods. Nevertheless, we are concerned about the susceptibility to bias that might creep in if we optimize scatter with respect to the parameters we seek to measure, so we choose to use medians, a simple and robust combination scheme. Our "best distance" for each SN Ia is just the median of all the distances of all the different methods (excepting redshift-based luminosity distance!). The best distances for the fall 1999 data presented here differ slightly from those in Table 6 because we did not have Δm_{15} distances for more than the fall 1999 data, and we thought that for the sake of consistency we should treat the fall 1999 data in the same way as the other SNe Ia for which we have observations. The scatter between the distances in Table 6 and Table 8 is 0.08 mag.

Obtaining accurate uncertainties is somewhat more complicated. The scatter of any method's results around any cosmological model may not match the error estimates. We therefore examine this scatter for each method, prune at 3 σ, and multiply the error estimates for each method by a factor to bring them into agreement with the scatter. This appears to be a more realistic adjustment than adding a "cosmic scatter" in quadrature (which we already do anyway when called for). We then obtain a final error estimate as the median of all of the contributing methods' errors diminished by the $\frac{1}{4}$ power of the number of contributors (a factor empirically derived by examining scatter around cosmological models). As above, we believe the covariance between the different methods applied to the same data is such that we are getting only a minimal improvement in accuracy by taking a median, but we hope that we are thereby "Gaussianizing" the distribution. The final list comprises 230 SNe Ia.

We use this list below for determining cosmological parameters, and although we will not repeat the data we found in the literature, we thought it important to publish the actual distances that are being used to calculate cosmological parameters as well as other relevant information which may be of use to others. In Table 8 we list the supernova name, its Galactic coordinates, host, and literature reference. We give the redshift as $\log(cz)$ and the luminosity distance and error in the same units, i.e., we do *not* want to use uncertain units of Mpc when we know the Hubble flow zero point so exquisitely well. The median of the estimates for host-galaxy extinction in the rest-frame V band follows, where we have used a standard Cardelli et al. (1989) extinction law to bring estimates in different bandpasses to V. Finally we identify the methods which contributed to the median: MLCS98 = R, SCP/stretch = P, MLCS2k2 = J, dm15 = S, and BATM = T.

4. COSMOLOGICAL IMPLICATIONS

4.1. *Hubble Diagrams*

At a redshift of 0.5, the difference in luminosity distance between a flat and open universe with $\Omega_M = 0.3$ is 0.22 mag. With 230 SNe Ia and 79 at redshifts greater than 0.3, we might expect to be able to distinguish between these cosmologies at better than 6 σ. The real concern, however, is whether we are making a systematic error or hitting a systematic noise floor for SNe Ia, and that we are fooling ourselves in thinking that we are making progress by averaging together more and more SNe Ia.

The goal of this particular campaign was to strive to find and follow SNe Ia at distinctly higher redshift than the majority of results at $z = 0.5$, since the effect of a dark-energy–dominated cosmology looks very different from most plausible systematic effects at $z \approx 1$. If the universe really has no dark energy and the dimness of SNe Ia by 0.22 mag at $z = 0.5$ is the result of a systematic error proportional to the redshift, one might expect SNe Ia to be dimmer by 0.44 mag at $z = 1$ instead of 0.26 mag, which would be the case for a flat universe.

Figure 8 shows the results from this campaign plotted over the full set of data from Table 8. Evidently there is a tendency for the SNe Ia to be brighter at $z > 0.9$ (although the uncertainties are still large), suggesting that we are truly

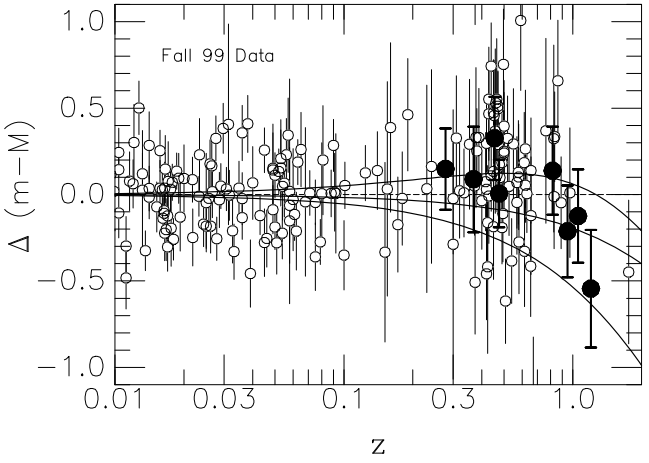

FIG. 8.—Fall 1999 and other data points in a residual Hubble diagram with respect to an empty universe. From top to bottom the curves show $(\Omega_M,\ \Omega_\Lambda) = (0.3,\ 0.7)$, (0.3, 0.0), and (1.0, 0.0), respectively, and the fall 1999 points are highlighted.

seeing a change in the deceleration of the universe and the effects of dark energy.

Given the heterogeneous nature of the data and the continual worry about non-Gaussian distributions, it is difficult to be quantitative about how well we can reject the possibility that we are seeing a systematic error in SN Ia brightness in a universe with no dark energy, and we discuss this in more detail below.

The scatter of the points from Table 8 obscures the trend with redshift, so we take medians over redshift bins and illustrate the result in Figure 9. Our redshift bins are derived from the data by choosing bins that have at least 12 SNe Ia and a bin width of more than 0.25 in $\log z$ but no more than 50 SNe Ia. The uncertainties, estimated from the 68% percentiles of the scatter of the points in each bin, are all less than 0.05 mag except for 0.08 mag in the highest z bin. We believe that this is approximately where systematics will start to dominate statistical error. That the points mostly lie below the (0.3, 0.7) cosmology gets at the heart of what we

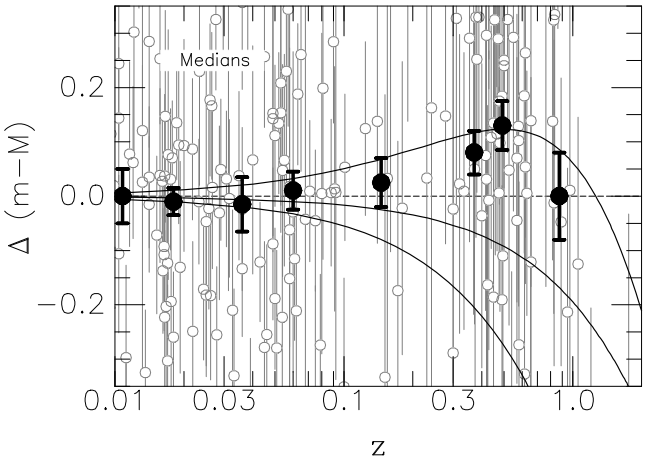

FIG. 9.—Fall 1999 and other data points in a residual Hubble diagram with respect to an empty universe. In this plot the highlighted points correspond to median values in eight redshift bins. From top to bottom the curves show $(\Omega_M,\ \Omega_\Lambda) = (0.3,\ 0.7)$, (0.3, 0.0), and (1.0, 0.0), respectively.

believe may the systematic uncertainty floor of the SN Ia distances in Table 8; we discuss this below. Nevertheless, we are apparently starting to see SNe Ia become brighter at $z \approx 0.9$, rather than becoming ever dimmer because of a systematic effect.

4.2. *Cosmological Parameters*

We can fit the data from Table 8 with a variety of cosmological models. We do not want to fit all 230 SNe Ia because the nearby ones are affected by peculiar motions, which are beyond the scope of this paper to characterize. However, we do need to allow for the velocity uncertainty in modeling, so when we compute χ^2 we add 500 km s^{-1} divided by the redshift in quadrature to the distance error. For all fits we report χ^2 at the minimum as a function of H_0, since this is equivalent to marginalizing over H_0.

Fitting all 230 SNe Ia yields $\chi^2 = 252$. If we restrict our fits to $z > 0.01$, we obtain $\chi^2 = 206$ for 195 points. We are also very wary of "extinguished" SNe Ia, since we are not certain we understand host extinction and reddening very well,[19] and we are mindful of the covariance between A_V and d. If we further restrict the sample to $A_V < 0.5$ mag we get $\chi^2 = 169.5$ for 172 SNe Ia, and we regard this as the most useful sample for deriving cosmological parameters. There are further cuts that could be made: exclusion of the SCP data points (where there is no information on host galaxy extinction) gives us $\chi^2 = 121.6$ for 130 SNe Ia. However, the constraints on cosmological parameters do not change significantly, and we are concerned about acquiring systematic problems along with spurious precision.

In the analyses that follow we use various subsamples of the 172 SNe Ia with $z > 0.01$ and $A_V < 0.5$ mag. For each calculation we determine χ^2 as a function of H_0, Ω_M, and Ω_Λ. Given that χ^2/N is close to unity, we convert this to a probability as $\exp(-0.5\chi^2)$, normalize, marginalize over H_0, and locate contours of constant probability density that enclose 68%, 95%, and 99.5% of the probability. In those calculations where we additionally constrain cosmology by using the galaxy clustering shape measurements, we use observations from the Two Degree Field (2dF) Redshift Survey (Percival et al. 2001), $\Omega_M h = 0.20 \pm 0.03$, and $H_0 = 72 \pm 8$ km s^{-1} Mpc^{-1} (Freedman et al. 2001). In all cases, contours are calculated for a cosmological constant equation of state ($w = -1$).

Figure 10 shows these contours for a sample of 94 SNe Ia ($\chi^2 = 103$), which include only the recent results from B. Leibundgut et al. (2003, in preparation), N. Suntzeff et al. (2003, in preparation), S. Jha et al. (2003a, in preparation), and the data presented here. The error ellipses are virtually

[19] Phillips et al. (1999) give in their Table 2 the Galactic and host reddening $E(B-V)$ for nearby supernovae. If, as suggested by the 44 SNe Ia studied by Jha (2002, § 3), most SNe Ia obey Lira's (1995) relation, then the colors at maximum and in the tail of the $B-V$ color curve *can* give us a good handle on the *reddening* at optical wavelengths. However, while most galaxies may have dust like that in our Galaxy, with $R_V \equiv A_V/E(B-V) \approx 3.1$ (Cardelli, Clayton, & Mathis 1989), there are heavily reddened objects such as SN 1999cl whose host galaxy has dust with $R_V < 2$ (Krisciunas et al. 2001). Furthermore, high-redshift supernovae are typically too faint to detect with sufficient precision 30 to 90 rest-frame days after maximum light. Finally, while a combination of optical and infrared data gives us a good handle on the extinction A_V (Krisciunas et al. 2000, 2001, 2003), SN Ia with $z \gtrsim 0.10$ are too faint in the rest-frame H- and K-band even for 10 m class telescopes to apply the V minus infrared method of determining extinction.

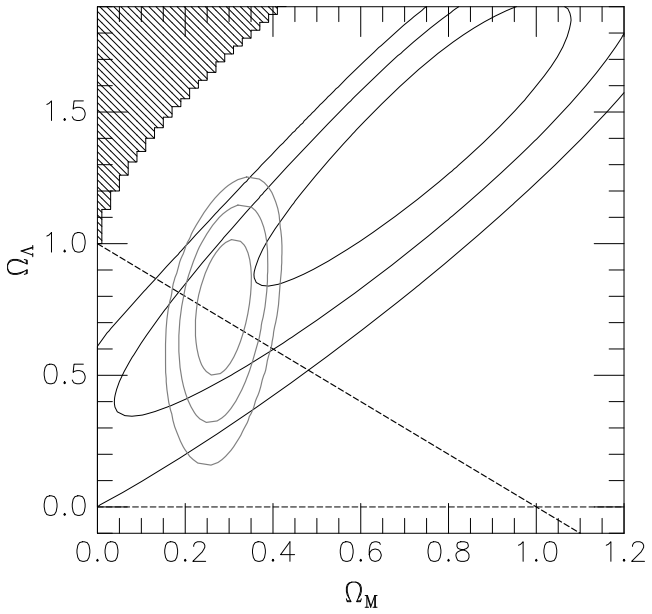

FIG. 10.—Probability contours for Ω_Λ vs. Ω_M, shown at 1, 2, and 3 σ with $w = -1$. We also give 1, 2, and 3 σ contours when we adopt a prior of $\Omega_M h = 0.20 \pm 0.03$ from the 2dF survey (Percival et al. 2001). These constraints use only the 26 new SNe Ia at $z > 0.3$ (which are completely independent of any which have been used before for cosmological constraints).

identical to those drawn by Riess et al. (1998a) and Perlmutter et al. (1999), although the data and analyses are completely different, confirming the conclusion that the universe is accelerating. This independent sample gives a consistent result: the acceleration inferred several years ago was not a statistical fluke.

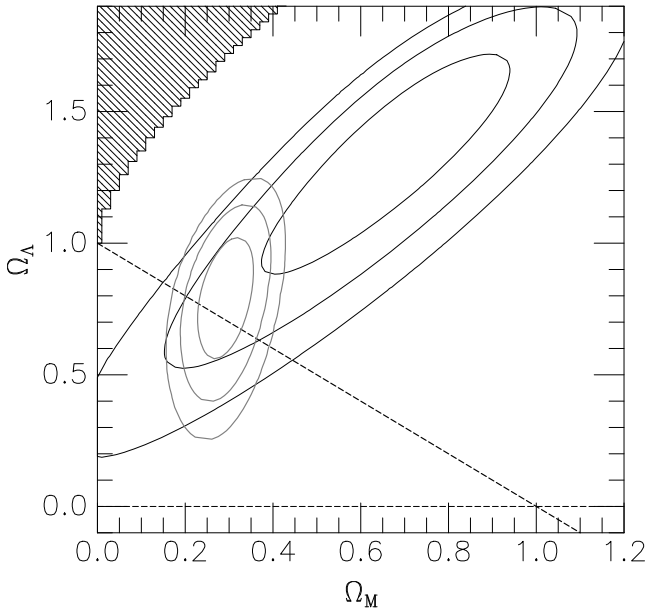

FIG. 11.—Probability contours for Ω_Λ vs. Ω_M, shown at 1, 2, and 3 σ with $w = -1$. We also give 1, 2, and 3 σ contours when we adopt a prior of $\Omega_M h = 0.20 \pm 0.03$ from the 2dF survey (Percival et al. 2001). These constraints use the 113 SNe Ia published by the HZT.

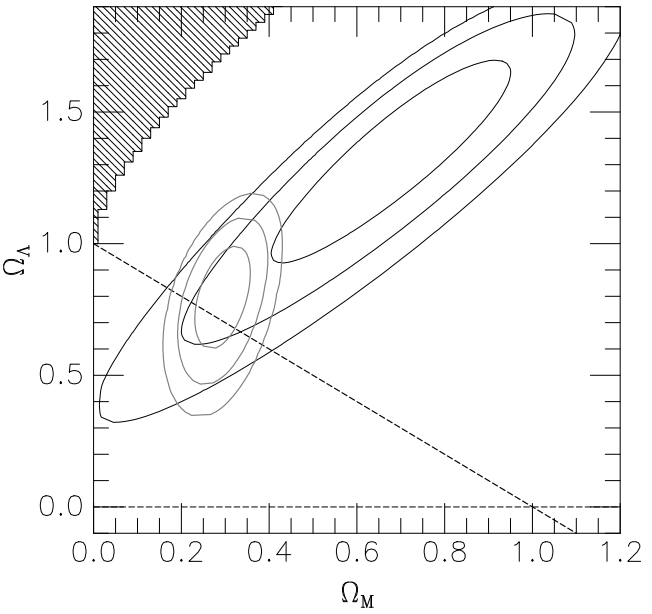

FIG. 12.—Probability contours for Ω_Λ vs. Ω_M, shown at 1, 2, and 3 σ with $w = -1$. We also give 1, 2, and 3 σ contours when we adopt a prior of $\Omega_M h = 0.20 \pm 0.03$ from the 2dF survey (Percival et al. 2001). These constraints use the full sample of 172 SNe Ia with $z > 0.01$ and $A_V < 0.5$ mag.

Figure 11 shows these contours for the sample of 130 SNe Ia ($\chi^2 = 122$), which includes all the SNe Ia that have been published by the HZT.

Figure 12 shows these contours for the sample of 172 SNe Ia ($\chi^2 = 170$), which includes all the SNe Ia for which we have either data or published results.

In all cases, the derived probability contours with a 2dF prior are remarkably tightly constrained to the $\Omega_{\rm tot} = 1$ line that is being delineated so well by CMB observations.

As with previous results from SNe Ia, the approximate combination $\Omega_\Lambda - \Omega_M$ is relatively well constrained. For these data

$$\Omega_\Lambda - 1.4\Omega_M = 0.35 \pm 0.14 \, .$$

However, the presence of these higher redshift observations from fall 1999 as well as SN 1997ff (Riess et al. 2001) has started to close off the contours from running away to very large Ω. If we assume a flat universe as well as $w = -1$, the SN Ia data require $\Omega_M = 0.28 \pm 0.05$, independent of large-scale structure estimates.

We can also fit for the equation of state of the dark energy, $p = w\rho$, where $w = \frac{1}{3}$ for radiation, $w = 0$ for pressureless matter (e.g., cold dark matter), $w = -1$ for a cosmological constant, etc. Restricting ourselves to $\Omega_{\rm tot} = 1$, Figure 13 shows the contours for Ω_M and w, with and without the 2dF prior.

Dark energy candidates with $w > -\frac{2}{3}$ are strongly disfavored by these data. Figure 14 shows the data from Figure 13 marginalized over Ω_M. The combination of SNe Ia and constraints on Ω_M from large-scale structure puts a sharp constraint on how positive w can be. The 95% confidence limits on w lie in the range $-1.48 < w < -0.72$. If we additionally adopt a prior that $w > -1$, we find that $w < -0.73$ at 95% confidence. These constraints are again very similar to recent results reported using the *WMAP* satellite:

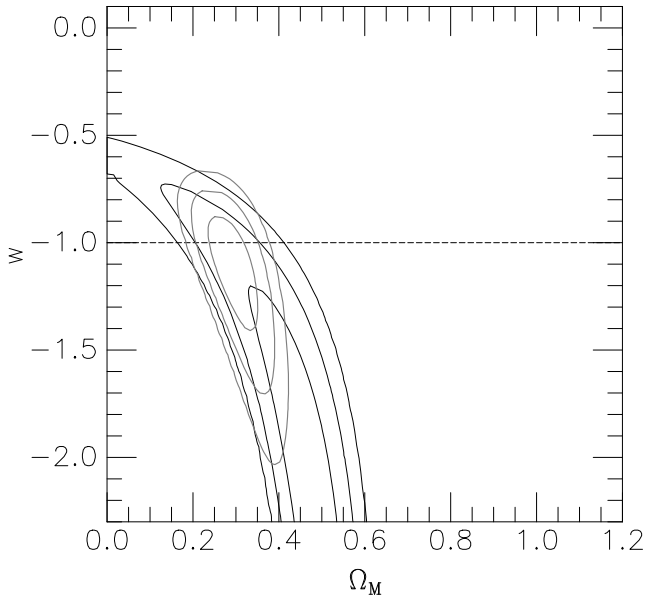

FIG. 13.—Probability contours for dark energy parameter w vs. Ω_m, shown at 1, 2, and 3 σ when $\Omega_{\rm tot} = 1$. We also give 1, 2, and 3 σ contours when we adopt a prior of $\Omega_M h = 0.20 \pm 0.03$ from the 2dF survey (Percival et al. 2001). This sample includes all 172 SNe Ia with $z > 0.01$ and $A_V < 0.5$ mag.

$w < -0.78$ at 95% confidence for priors of $w > -1$ and Ω_M from the 2dF Redshift Survey (Spergel et al. 2003).

Since the gradient of $H_0 t_0$ is nearly perpendicular to the narrow dimension of the Ω_Λ-Ω_M contours, we obtain a surprisingly good estimate of $H_0 t_0$, illustrated in Figure 15. We find that $H_0 t_0 = 0.96 \pm 0.04$. Although independent measurements of these parameters do not approach this precision yet, for comparison we note that $h = 0.72 \pm 0.08$ from Freedman et al. (2001) corresponds to a Hubble time of $H_0^{-1} = 13.6 \pm 1.5$ Gyr. Krauss & Chaboyer (2003) have recently found a median age of 12.5 Gyr for 17 metal-poor globular clusters. If these globular clusters formed 0.6 Gyr after the big bang, then the universe has $t_0 = 13.1$ Gyr, consistent with a world model with $h = 0.72$, $\Omega_M = 0.3$, and

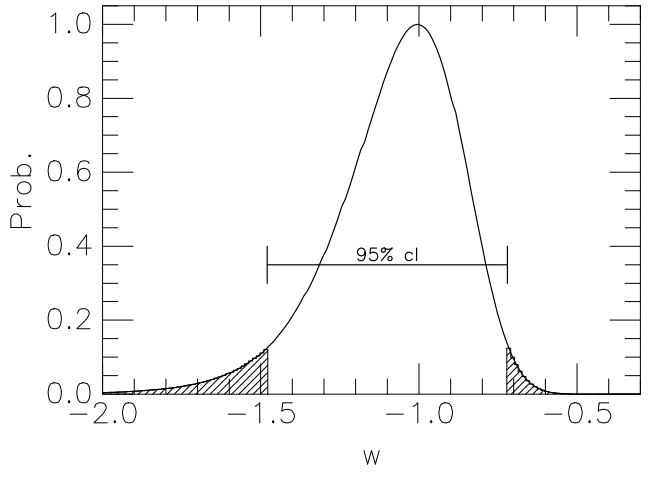

FIG. 14.—Probability distribution for w using the 2dF prior, marginalized over Ω_M. The 95% confidence limits are $-1.48 < w < -0.72$.

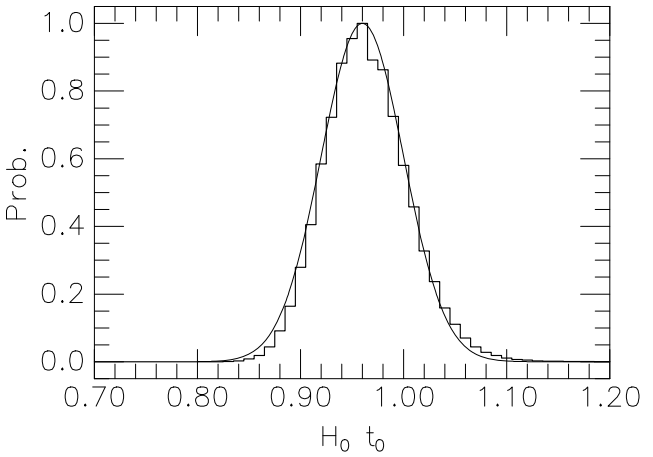

FIG. 15.—Probability distribution for $H_0 t_0$ given the SN Ia observations is tightly constrained to 0.96 ± 0.04, and an approximating Gaussian curve.

$\Omega_\Lambda = 0.7$. The assumed globular cluster incubation time of 0.6 Gyr corresponds to an epoch of star formation we would observe now at $z \approx 8$. Adopting an uncertainty of ± 2 Gyr for t_0, the product $H_0 t_0 = 0.96 \pm 0.19$. We also note that remarkable agreement with the *WMAP* result for the age of the universe: 13.7 ± 0.2 Gyr (Spergel et al. 2003).

5. DISCUSSION

5.1. *Testing Systematics*

Drell et al. (2000, hereafter DLW) wrote a very thoughtful critique of the then extant SN Ia data, questioning whether a cosmological constant was required or a systematic error could account for the observations. We here present more than twice as many objects with improved error estimates. We believe that some of the points noted by DLW are simply caused by selection effects, for example the observed diminution of the range of Δ with redshift. However, their point that a large systematic shift in the luminosity of supernovae with redshift, coupled with a large positive Ω_M, could fit the data nearly as well as a universe with a cosmological constant, is still valid.

Using our preferred sample of 172 SNe Ia we reevaluate the Bayesian odds factor between a model "FRW" with no systematic error and a cosmological constant and a "Model II" with no cosmological constant but a systematic error that scales as a power law of $(1 + z)$ (i.e., the distance modulus has a systematic error term of $\beta \ln(1 + z)$—this is the DLW Model II). When we integrate both models over H_0, Ω_M, and either Ω_Λ or β and divide by plausible prior ranges for these parameters, we get an odds factor of 29 in favor of the FRW model. Most would interpret this as "pretty good" odds that the FRW model is to be preferred over a systematic error, but not extremely strong odds.

However, in this Bayesian framework, the ratio of the probabilities for the two models also includes the ratio of the prior probabilities. The systematic model can match the observations reasonably well, but it does so only for $\Omega_M \approx 1$ and a β that corresponds to a systematic that rises to 0.7 mag at $z = 1$. Both of these parameters seem out of step with other lines of investigation and would be quite disfavored by reasonable priors.

We certainly do not expect that Ω_M could be anywhere near unity. The evidence against this comes from the observations that the $H_0 t_0$ product appears to be much larger than $\frac{2}{3}$, and there is ample evidence on many scales that there is nowhere near as much mass as $\Omega_M = 1$ in clustered form (e.g., Blakeslee et al. 1999; Percival et al. 2001).

The argument against such a very large systematic error (0.7 mag at $z = 1$) is theoretical and empirical. We work with SNe Ia precisely because they are dead stars which should show very little difference between today and 7 Gyr ago, and we certainly do not have any theoretical expectation that explosions have become a factor of 2 dimmer in the mean over the previous 7 Gyr.

Empirically, we argue that the SNe Ia we see locally should have at least the range of properties seen at $z = 1$ because there are low-metallicity systems today and there appear to be SNe Ia that are exploding quite promptly (e.g., NGC 5253 at $0.1L^*$ had a starburst recently and has had two SNe Ia in the past century). Likewise, if SNe Ia were as much as a factor of 2 dimmer in the past, we would expect there to be a significant dispersion—surely *some* of the SNe Ia at $z = 1$ would produce explosions comparable to those of today.

We are always cognizant of the possibility of observational systematic error or problems with our analysis, but 0.7 mag is considerably beyond what we think might be possible.

The exact factor by which Model II would therefore be disfavored according to these prior considerations is subjective, since the place where the systematic probability becomes sizable is out on the tails of the priors we assign for Ω_M and β. We think it is not worthwhile to try to assign a quantitative probability to these, other than to note that the factor by which the net probability of Model II relative to the FRW model will be disfavored will be significantly higher than the factor of 29 from the integrated likelihoods.

Therefore, we believe that we have very strong evidence that a systematic effect that scales as a power law of $(1 + z)$ is not likely to match the SN Ia data. In particular, a simple gray or intergalactic dust model does not appear to be viable, and evolutionary effects such as metallicity, C/O ratio, or host dust properties that change smoothly and monotonically with z are also likely not to fit the data as well as an FRW cosmology.

It is always possible to imagine a systematic error that is tuned to match the FRW turnover near $z = 1$, but it might be a priori less plausible than a simple $(1 + z)$ power. However, a proper Bayesian analysis would have to take into account the volume of the space from which such a model was drawn, and the model might be disfavored for that reason, even though it might fit the SN Ia data very well.

5.2. *Selection and Other Effects*

The fall 1999 survey went deeper and redder than any previous campaign. As a result, we did start to see extinguished SNe Ia at $z \approx 0.5$ and we expect that we are less subject to selection bias.

Our model for rates seems to work remarkably well, suggesting that there is not a rare population of luminous objects that we do not know about from local samples. The exceptions are SN 1999fo (Gertie) and SN 1999fu (Alvin), which were not SNe Ia, but were definitely unusual, flux-variable objects.

At face value, the average absorption of the distant supernovae is significantly smaller than for the nearby sample. Out to $z \leq 0.3$, the 151 supernovae suffered an average absorption of $\langle A_V \rangle = 0.35 \pm 0.50$ mag, while the 37 distant supernovae with $z > 0.3$ average $\langle A_V \rangle = 0.20 \pm 0.23$ mag. There is a large scatter in these averages, but the offset is 0.15 mag. The distribution of absorption values for the nearby supernova sample has a long tail to higher absorptions, which is missing for the distant sample. However, the distribution of absorptions of the distant supernovae is much narrower. Most probably this is a signature of the magnitude-limited searches, where heavily obscured supernovae are not detected. Selecting the 130 objects (172 less 42 SCP SNe Ia without host extinctions) that were used to construct the likelihood functions ($z > 0.01$ and $A_V < 0.5$ mag), we find that the averages decrease to $\langle A_V \rangle = 0.17 \pm 0.14$ mag for the nearby supernovae and $\langle A_V \rangle = 0.14 \pm 0.11$ mag for the distant ones. The difference has decreased to less than 0.03 mag, and clearly the faintness of the distant supernovae cannot be attributed to errors in the treatment of absorption. In fact, more absorption would make the distant supernovae more luminous and move them to larger distances. The small average absorption argues that the distant objects indeed are at larger distances than for an empty universe model, in agreement with the results from Riess et al. (2000), Leibundgut (2001), and Sullivan et al. (2003).

Of the objects at $z > 0.8$ in our large data set, several objects (principally those discovered before 1999) rely on rest-frame U-band data to measure extinction. The rest-frame U-band data have a number of uncertainties, including less certain K-corrections, greater susceptibility to extinction, and less well studied behavior. Most importantly, the SNe Ia have less intrinsic uniformity in the U bandpass. For the data set presented here, the average measured distance to those objects using the U band as a primary source of information for distance measurement is farther than to those objects that do not rely on U-band data, but the difference is not statistically significant. These effects will be further discussed in S. Jha et al. (2003a, in preparation) and N. Suntzeff et al. (2003, in preparation).

We have not corrected these data for gravitational lensing. It should be negligible at these redshifts, but will become much more serious as we push to higher redshift.

Nevertheless, we do think we can start to perceive systematic errors in the data at the 0.04 mag level. The contours seen in Figures 10–12 have their most probable Ω_M, Ω_Λ well offset from the Ω_M indicated by the 2dF survey and a flat universe. This is not a failure of our probability analysis. We have performed extensive Monte Carlo tests on simulated data sets, and we recover Ω_M, Ω_Λ with very little bias. What drives our best-fit solution to high values of Ω_M, Ω_Λ is the fact that the data make a very fast transition from recent acceleration to earlier deceleration, i.e., the transition from the faintness at $z \sim 0.5$ to the brightness at $z \sim 1$ is very fast. The contours in Figures 10–12 are quite shallow in the $\Omega_M + \Omega_\Lambda$ direction, and a systematic error of 0.04 mag is quite sufficient to move our most probable values for Ω_M, Ω_Λ to these high values. This may be a statistical fluke at the 1.5 σ level, although the systematic offsets of the points in Figure 9 from a cosmological line may point to systematic errors.

We have described some of the possible culprits for such a systematic above. Selection biases because of UV selection

or any of the other practical difficulties in carrying out a supernova search are always a worry, particularly since they are so hard to quantify and because SNe Ia are so nonuniform in the UV. Photometric and *K*-correction errors are certainly possible, since absolute photometry of objects with nonstellar SEDs at $m > 20$ is *extremely* hard to achieve at the 0.01 mag level. It is conceivable that gravitational lensing is more important than has been estimated; we expect that the SNe Ia found by the GOODS survey will offer a strong test of this. Most likely there is a variety of errors throughout this very heterogeneous set of data, and the best way forward is acquisition of new data from well-designed observations that are taken and analyzed with more care. Although the basic conclusion that the universe is accelerating is not in jeopardy, since the Ω_M-Ω_Λ direction is relatively insensitive to systematic error, we remain wary of overinterpretation of the extant SN Ia data and urge others to do the same.

5.3. *Comparison with the CMB*

As this paper was nearing completion, the *WMAP* team reported new results from a high angular resolution all-sky map of structure (Spergel et al. 2003). Their main conclusions, namely that we live in a geometrically flat universe with $\Omega_{\rm tot}$, Ω_M, and Ω_Λ of 1.00, 0.73, and 0.27, respectively, are entirely consistent with the results presented here. This convergence of results lends great strength to what is emerging as the new "standard model" of contemporary cosmology, in which the role of matter is secondary to the accelerating expansion driven by dark energy.

Ascertaining the physical mechanism that is responsible for this accelerating expansion is one of the crucial next steps for observational cosmology. Since supernovae are well suited to probing precisely the redshift range over which Λ begins to dominate, new projects are being undertaken to exploit this.

5.4. *What Next? The Future*

Future campaigns to observe SNe Ia at high redshift will focus on three themes: refining measures of luminosity distance, understanding and controlling systematic errors, and learning about SN Ia physics. The payoff for measuring luminosity distances accurately is that we can determine the equation of state of the dark energy and whether it has changed as a function of time (redshift). There is certainly a systematic floor to our ability to determine distances from SNe Ia, but we do not yet know what it is. It appears that gray dust is not an issue, but gravitational lensing, for example, is certainly a contaminant.

Opinions differ as to where the incompletely understood SN Ia physics causes a cosmic scatter that does not average out, but most would agree it lies in the range of 0.02–0.04 mag. This implies that the luminosity distance at a given redshift is not improved by observing more than 25–100 SNe Ia at that redshift. There are many outstanding questions about SN Ia physics, which may best be approached by observations of SNe Ia at high redshift. Measuring SN Ia rates and comparison with the star formation rate may elucidate the SN Ia explosion mechanism, SN Ia progenitors, and gestation period. The distribution of SN Ia parameters as a function of redshift may also be useful for understanding SN Ia and host galaxy physics.

The HZT, in collaboration with the Surf's-Up group at the Institute for Astronomy (IfA), Hawaii, undertook a 6 month survey of 2.5 deg^2 in *R*, *I*, and *Z*. Many SNe Ia as well as other transient objects were discovered and followed (Barris et al. 2002). Members of the HZT have begun the ESSENCE survey (Smith et al. 2002) to discover and follow 200 SNe Ia in the range $0.1 < z < 0.8$ with the goal of measuring the equation of state parameter w of the dark energy to $\pm 10\%$. Riess et al. (2003) have an ongoing program with *HST* and the GOODS survey, using the Advanced Camera for Surveys (ACS) to discover and follow approximately six SNe Ia at $z \approx 1.4$. This will be exceedingly powerful for measuring the effects of dark energy, understanding systematics, and constraining any time evolution of w. The CFHT Legacy Survey[20] has the goal of finding and following $\sim$2000 SNe Ia in multiple colors. The Lick Observatory Supernova Search (LOSS; Filippenko et al. 2001) is finding and monitoring record numbers of very nearby supernovae, with 82 in 2002 alone.[21] The Nearby Supernova Factory (Aldering et al. 2002) will obtain spectrophotometry for $\sim$300 nearby SNe Ia, suitable for *K*-corrections of high-redshift supernovae and for exploring SN Ia physics and systematics. In the near future, Pan-STARRS (Kaiser et al. 2002) should discover and follow a vast number of SNe Ia ($>10^4$ per year). Finally, in the more distant future, the proposed *SNAP* satellite (Nugent 2001) would follow several thousand objects with an experiment designed to minimize observational systematic errors, limited only by the floor imposed by nature. The future indeed looks bright for cosmological and related studies of SNe Ia.

We thank the staffs at many observatories for their assistance with the observations. Financial support for this work was provided by NASA through programs GO-08177, GO-08641, and GO-09118 from the Space Telescope Science Institute, which is operated by the Association of Universities for Research in Astronomy, Inc., under NASA contract NAS 5-26555. Funding was also provided by National Science Foundation grants AST 99-87438 and AST 02-06329. A. C. acknowledges the support of CONICYT (Chile) through FONDECYT grants 1000524 and 7000524. This paper uses data from the Sloan Digital Sky Survey (SDSS) early data release.

[20] See http://www.cfht.hawaii.edu/Science/CFHLS.
[21] See http://astro.berkeley.edu/~bait/kait.html.

APPENDIX

$N(N-1)/2$ DIFFERENCES

We use the Alard & Lupton (1998) code to convolve one image to match the other. We fit a suitable star in one of these images with the Schechter "Waussian" (inverse of a truncated Taylor series for e^{x^2}) to derive a standard PSF. Since we know where the supernova is located, we do a two-parameter fit (peak and sky) of this standard PSF, and we scale the flux measured in the standard star by the ratio of the fit peaks to derive a supernova flux difference for these two images. We also select roughly 10 other locations in the image and insert a copy of the standard star scaled to match the supernova flux, and pick it up again using the same procedure of two-parameter fits. This tells us of any bias (we do not see any) and gives us an estimate of the flux error for this pair of images.

Applying this procedure to all $N(N-1)/2$ pairs creates an $N \times N$ antisymmetric matrix of flux differences, and a symmetric matrix of errors. We also choose approximately a dozen stars for each supernova field that are bright enough to have good S/N in all images but faint enough not to be saturated, and perform a PSF flux measurement for all stars in all images. Matching up these tables of stars, we can form a mean flux scale between all pairs of images, and then assemble another $N \times N$ antisymmetric matrix of magnitude differences. The flux differences are all put on a common scale using the magnitude differences.

Finally, we fit these antisymmetric matrices as the difference between the ith and jth entries of an N vector. We derive two sets of error estimates: the first is based on the pairwise flux error estimates, and the second comes from the residuals between the observed difference matrix and the matrix assembled by differencing the terms of the resulting vector. These estimates are generally consistent with one another, although the observed errors reflect the uncertainties of the individual observations and the mismatch errors give a broader view of the inconsistency of any observation with the others.

REFERENCES

Aguirre, A. 1999a, ApJ, 512, L19
———. 1999b, ApJ, 525, 583
Alard, C., & Lupton, R. H. 1998, ApJ, 503, 325
Aldering, G., et al. 2002, Proc. SPIE, 4836, 61
Barris, B., et al. 2002, BAAS, 34, 1306
Benítez, N., Riess, A., Nugent, P., Dickinson, M., Chornock, R., & Filippenko, A. V. 2002, ApJ, 577, L1
Blakeslee, J. P., Davis, M., Tonry, J. L., Dressler, A., & Ajhar, E. A. 1999, ApJ, 527, L73
Buta, R. J., & Turner, A. 1983, PASP, 95, 72
Candia, P., et al. 2003, PASP, 115, 277
Cappellaro, E., Evans, R., & Turatto, M. 1999, A&A, 351, 459
Cardelli, J. A., Clayton, G. C., & Mathis, J. S. 1989, ApJ, 345, 245
Carroll, S. M. 2001, Living Rev. Relativ., 4, 1
Coil, A. L., et al. 2000, ApJ, 544, L111
Cousins, A. W. J. 1976, MmRAS, 81, 25
de Bernardis, P., et al. 2002, ApJ, 564, 559
Dolphin, A. E. 2000, PASP, 112, 1397
Drell, P. S., Loredo, T. J., & Wasserman, I. 2000, ApJ, 530, 593 (DLW)
Falco, E. E., et al. 1999, ApJ, 523, 617
Farrah, D., Meikle, W. P. S., Clements, D., Rowan-Robinson, M., & Mattila, S. 2002, MNRAS, 336, L17
Filippenko, A. V. 1997, ARA&A, 35, 309
Filippenko, A. V., Li, W. D., Treffers, R. R., & Modjaz, M. 2001, in ASP Conf. Ser. 246, Small-Telescope Astronomy on Global Scales, ed. W. P. Chen, C. Lemme, & B. Pacynski (San Francisco: ASP), 121
Filippenko, A. V., & Riess, A. G. 2001, in Particle Physics and Cosmology: Second Tropical Workshop, ed. J. F. Nieves (New York: AIP), 227
Filippenko, A. V., et al. 1992, AJ, 104, 1543
———. 1995, ApJ, 450, L11
Folkes, S., et al. 1999, MNRAS, 308, 459
Ford, C. H., et al. 1993, AJ, 106, 1101
Freedman, W., et al. 2001, ApJ, 553, 47
Garnavich, P. M., et al. 1998a, ApJ, 493, L53
———. 2001, preprint (astro-ph/0105490)
Germany, L. M. 2001, Ph.D. thesis, Australian National Univ.
Germany, L. M., et al. 2003, A&A, in press
Hamuy, M., Phillips, M. M., Maza, J., Suntzeff, N. B., Schommer, R. A., & Avilés, R. 1995, AJ, 109, 1
Hamuy, M., Phillips, M. M., Suntzeff, N. B., Schommer, R. A., Maza, J., Smith, R. C., Lira, P., & Avilés, R. 1996a, AJ, 112, 2438
Hamuy, M., et al. 1991, AJ, 102, 208
———. 1996b, AJ, 112, 2408
Hatano, K., Branch, D., & Deaton, J. 1998, ApJ, 502, 177
Höflich, P., Wheeler, J. C., & Thielemann, F.-K. 1998, ApJ, 495, 617
Jha, S. 2002, Ph.D. thesis, Harvard Univ.
Jha, S., et al. 1999, ApJS, 125, 73
Kaiser, N., et al. 2002, Proc. SPIE, 4836, 154
Kim, A., Goobar, A., & Perlmutter, S. 1996, PASP, 108, 190
Kirshner, R. P., et al. 1993, ApJ, 415, 589
Krauss, L. M., & Chaboyer, B. 2003, Science, 299, 65
Krisciunas, K., Hastings, N. C., Loomis, K., McMillan, R., Rest, A., Riess, A. G., & Stubbs, C. 2000, ApJ, 539, 658
Krisciunas, K., et al. 2001, AJ, 122, 1616
———. 2003, AJ, 125, 166
Kron, G. E., & Smith, J. L. 1951, ApJ, 113, 324
Landolt, A. U. 1992, AJ, 104, 340
———. 2001, ARA&A, 39, 67
Leibundgut, B., Tammann, G. A., Cadonau, R., & Cerrito, D. 1991, A&AS, 89, 537
Leibundgut, B., et al. 1993, AJ, 105, 301
Li, W. D., Filippenko, A. V., Treffers, R. R., Riess, A. G., Hu, J., & Qiu, Y. 2001a, ApJ, 546, 734
Li, W. D., et al. 1999, AJ, 117, 2709
———. 2001b, PASP, 113, 1178
Lira, P. 1995, MA thesis, Univ. Chile
Lira, P., et al. 1998, AJ, 115, 234
Mandel, K., et al. 2001, BAAS, 199, 4704
Marzke, R. O., da Costa, L. N., Pellegrini, P. S., Willmer, C. N. A., & Geller, M. J. 1998, ApJ, 503, 617
Massey, P., Strobel, K., Barnes, J. V., & Anderson, E. 1988, ApJ, 328, 315
Meikle, P., et al. 1996, MNRAS, 281, 263
Modjaz, M., et al. 2001, PASP, 113, 308
Nørgaard-Nielsen, H. U., Hansen, L., Jorgensen, H. E., Aragon Salamanca, A., & Ellis, R. S. 1989, Nature, 339, 523
Novicki, M. C., & Tonry, J. 2000, BAAS, 32, 1576
Nugent, P. 2001, in Particle Physics and Cosmology: Second Tropical Workshop, ed. J. F. Nieves (New York: AIP), 263
Nugent, P., Kim, A., & Perlmutter, S. 2002, PASP, 114, 803
Oke, J. B., et al., 1995, PASP, 107, 375
Padmanabhan, T. 2002, preprint (hep-th/0212290)
Paerels, F., Petric, A., Telis, G., & Helfand, D. J. 2002, BAAS, 34, 1264
Pain, R., et al. 1996, ApJ, 473, 356
———. 2002, ApJ, 577, 120
Patat, F., et al. 1996, MNRAS, 278, 111
Peacock, J. A., et al. 2001, Nature, 410, 169
Percival, W. J., et al. 2001, MNRAS, 327, 1297
Perlmutter, S., et al. 1995, ApJ, 440, L41
———. 1997, ApJ, 483, 565
———. 1998, Nature, 391, 51
———. 1999, ApJ, 517, 565
Persson, S. E., Murphy, D. C., Krzeminski, W., Roth, M., & Rieke, M. J. 1998, AJ, 116, 2475
Phillips, M. M. 1993, ApJ, 413, L105
Phillips, M. M., Lira, P., Suntzeff, N. B., Schommer, R. A., Hamuy, M., & Maza, J. 1999, AJ, 118, 1766
Rana, N. C. 1979, Ap&SS, 66, 173
———. 1980, Ap&SS, 71, 123
Richmond, M. W., et al. 1995, AJ, 109, 2121
Riess, A. G. 2000, PASP, 112, 1284
Riess, A. G., Press, W. H., & Kirshner, R. P. 1995, ApJ, 438, L17
———. 1996, ApJ, 473, 88
Riess, A. G., et al. 1998a, AJ, 116, 1009
———. 1998b, ApJ, 504, 935
———. 1999a, AJ, 117, 707
———. 1999b, AJ, 118, 2675

Riess, A. G., et al. 2000, ApJ, 536, 62
———. 2001, ApJ, 560, 49
———. 2003, ApJL, in press
Rowan-Robinson, M. 2002, MNRAS, 332, 352
Savage, B. D., & Mathis, J. S. 1979, ARA&A, 17, 73
Schlegel, D. J., Finkbeiner, D. P., & Davis, M. 1998, ApJ, 500, 525 (SFD)
Schmidt, B. P., et al. 1998, ApJ, 507, 46
Smith, R. C., et al. 2002, BAAS, 34, 1232
Spergel, D. N., et al. 2003, ApJ, submitted
Stetson, P. B. 1987, PASP, 99, 191
Stetson, P. B., & Harris, W. E. 1988, AJ, 96, 909
Stoughton, C., et al. 2002, AJ, 123, 485
Sullivan, M., et al. 2003, MNRAS, 340, 1057
Suntzeff, N. B., et al. 1999, AJ, 117, 1175
Tonry, J., et al. 1999, IAU Circ. 7312
Tsvetkov, D. Yu. 1982, Soviet Astron. Lett., 8, 115
Turatto, M., et al. 1996, MNRAS, 283, 1
———. 1998, AJ, 116, 2431
Wells, L. A., et al. 1994, AJ, 108, 2233
Wilson, G., Cowie, L. L., Barger, A. J., & Burke, D. J. 2002, AJ, 124, 1258